國 立 交 通 大 學

環 境 工 程 研 究 所

碩士論文

利用溶膠−凝膠法製備高辨識能力的17β-estradiol分子拓印材料

Fabrication of 17β-estradiol imprinted silica with high recognition capability using a sol-gel method

研 究 生：侯精榮

指導教授：張淑閔 博士

中 華 民 國 九 十 九 年 一 月

中文摘要

17β-estradiol(E2)是內分泌干擾物中含苯環的類固醇荷爾蒙,對於野生動物及人類會造成內分泌系統干擾的負面影響,因此,針對E2 發展高效能偵測方法引起廣大興趣,分子拓印高分子對於目標分子具有高選擇性和親和性,是最新發展出篩選與濃縮標的物的重要材料,本研究目的為利用溶膠-凝膠法(sol-gel)製備和鑑定 17β-estradiol(E2)的分子拓印有機無機混合材料,並藉由材料與吸附能力分析了解分子拓印與最佳化製備條件。官能性單體苯基三甲氧基矽氧烷(PTMOS)和 3-氨基丙基三甲基矽氧烷(APTES)是用來當作官能性單體並分別藉由π-π作用力和氫鍵作用來和E2 產生鍵結。此外,四乙烷基矽烷(TEOS)當作交聯劑並建構多孔隙凝膠, 甲基三甲氧基矽烷(MTMOS)的添加可以增加材料的柔韌性。當TEOS/PTMOS/APTES/MTMOS/E2 莫爾比為 20:2:2:2:1 時,材料於乙腈中對E2 的吸附量為 0.36 mg E2/g MIPs而拓印因數為 1.8,其中,PTMOS和APTES分別決定材料的辨識力和吸附能量,當pH=3 和水/Si莫爾比值為=3.3 時,材料在乙腈中呈現最高吸附能力 0.44 mg E2/g MIPs和拓印因數 1.9,此外,分子拓印材料於甲苯溶劑中的吸附能力更提高至 28.2 mg E2/g MIPs。分子拓印材料在經過模板萃取之後,比表面積很明顯地從 288 m^2/g提高到 658 m^2/g,孔體積也從 0.25 cm^3/g提高到 0.59 cm^3/g,另外,分子拓印材料的吸附平衡時間為 4 小時。分子拓印材料對於 1-萘酚(1-naphthol)的選擇性(selectivity factor)為 3.1 而壬基苯酚(nonylphenol)的選擇性為 2.3,這些結果證明拓印作用確實藉由溶膠-凝膠法產生在有機無機混合材料上。

Abstract

17β-estradiol (E2) is a phenolic steroid hormone of endocrine disrupted contaminants. It has adverse effects and cause abnormality on the endocrine system of wildlife and humans. The high selectivity and affinity of molecularly imprinted polymers (MIPs) toward target molecules make them receive much attention on separation and sensing of E2. The aim of this study was to develop and characterize E2 imprinted organic-inorganic hybrid silica using a sol-gel process. Phenyltrimethoxysilane (PTMOS) and 3-aminopropyltriethoxysilane (APTES) were used as functional monomers to selectively bind E2 via π-π stacking interactions and hydrogen bonding, respectively. In addition, tetraethoxylsilane (TEOS) was used as a cross-linker to polymerize the highly porous gels. To enhance the mechanical elasticity, methyltrimethoxysilane (MTMOS) was incorporated into the gels. The recipes and sol-gel parameters were optimized to reach the highest imprinted capabilities. The imprinted material with the optimal TEOS/PTMOS/APTES/MTMOS/E2 molar ratio of 20/2/2/2/1 exhibited an adsorption capacity of 0.36 mg/g and an imprinted factor of 1.8 in acetonitrile. The PTMOS and APTES dominated the recognitions and binding quantities, respectively. The imprinted material showed the highest adsorption capacity of 0.44 mg/g and the imprinted factor of 1.9 in acetonitrile when the sol-gel process was proceeded at water/Si=3.3 and pH=3. Moreover, the adsorption capacity was remarkably enhanced to 28.2 mg/g in toluene. After removal of E2, the specific surface areas and pore volume of imprinted silica was increased significantly from 288 m^2/g to 658 m^2/g and 0.25 cm^3/g to 0.59 cm^3/g, respectively. In addition, the adsorption equilibrium time was 4 hr for the imprinted polymers. The imprinted silica performed high selectivity factor of 3.1 for 1-naphthol and 2.3 for nonylphenol in competitive adsorption systems. These results clearly demonstrated that the imprinted effect was successfully conducted in the organic-inorganic

silica hybrids through the sol-gel process.

誌謝

三年多的研究所生涯，終於告一段落。回首剛回到校園進修時的期待，以及現在收成的喜悅，這一切都要感謝許多人對我的提攜與幫助。

這一篇論文能夠順利完成，首先要感謝我的指導老師－張淑閏老師。在老師的教導下改變我對於做研究的態度。再來要感謝我的口試委員白曛綾教授、董瑞安教授和孫毓璋老師，在口試時對於我的指正和提供建議，讓我發現本論文主題可以更深入探討的地方，使本論文更加完善。

本論文的完成另外亦得感謝董老師實驗室的Michelle、Barry、Judy、Fio大力協助，因為有你們的幫忙，使得本論文能夠更完整。感謝Eric、Steel學長、Evelyn學姐們不厭其煩的指出我研究中的缺失，且總能在我迷惘時為我解惑，也感謝Wes、Claire、學詩、青洲、小小郭、小迪、范氏宗親、亮易同學的幫忙，使我的碩士生活一點也不孤單。實驗室的Adam、Ian、Ashley學弟、候鳥計畫的Charles以及Michelle、Joe、Karen、Jiphi學妹們當然也不能忘記，你們的幫忙及搞笑我銘感在心。此外YPHS-帥哥美女們的支援、CSJH-Josh的信心喊話，以及THU-時尚幫和卡達同學會當我的後盾，讓我有勇氣走完這全程，女朋友在背後的默默支持更是我前進的動力。

僅以本文獻給所有關心我與幫助過我的人。

精榮　謹誌

中華民國九十九年一月

Table of contents

Table captions

Figure Captions

IX

Chapter 1.   Introduction and Motivation

1-1   Motivation

Wide varieties of artificial chemicals having similar structure to endogenous hormone are currently manufactured and discharged into environment.   The chemicals which could interfere with normal function of the endocrine (hormone) system of humans and animals are called endocrine disrupting chemicals (EDCs).   17β-estradiol (E2) is one of nature hormones of EDCs and the structure of E2 is showed in Figure 1-1.   E2 can be toxic and carcinogenic to human body and inhibit egg implantation and impotence even at trace concentration levels.[1, 2]   It is reported that the feminization of male fish occurs when the concentration of E2 reaches 1-10 ng/L.[3]   Therefore, the monitoring of E2 is an important issue for environmental control of the compound.   The most commonly used methods for E2 determination are comprehend immune technique and instrumental analysis.[3-5]   However, biological test systems also have considerable limits on sensing toxic contaminants and low stability in harsh environment.   Although the instrument analysis has a good sensitivity to evaluate many pollutants in complicated mixtures, they need high cost, complicated pre-treatment, large amounts of organic solvents.[3, 6, 7]   Therefore, a methodology for recognition and quantification of E2 is highly demanded.

Molecular imprinted polymers (MIPs) are newly developed materials, which provides specific binding properties for separation and sensing.[8]   The imprinting mechanism is based on polymerization of self-assembled functional monomers-template complex in a facilitating solvent (porogen).   It remains specific cavity after removal of the template from network. The specific recognition binding of MIPs by structural similarity and functional groups can show high selectivity and affinity to target molecule.[7, 9, 10]   The uses of MIPs for sensing E2 has been published in many literatures.[5, 11, 12]   Highly dispersed E2-imprintedpolymers have

been prepared using ethylene glycol dimethacrylate (EDGMA) and 4-vinylpyridine (4-VP) as a cross-linker and a functional monomer, respectively.   It performed high imprinted factor of 4.22 due to the hydrophobic and hydrogen bonding interactions.[13]   Wei et al. have been fabricated E2-imprinted micro and nanospheres, and proved that the recognition of particles toward E2 was effective due to the binding to specific recognition sites.[14]   Although the organic MIPs have been well-established, they may shrink or swell when exposed to different mobile phase, and further change the essential of organic MIPs for recognition.   Compare to organic MIPs, organic-inorganic hybrid MIPs shows high chemical and thermal stability.

Sol-gel method has been widely used to synthesize organic-inorganic hybrid materials because it can easily adjust chemical compositions, microstructure, textures and be adapted at around room temperature.[15, 16, 17]   Sol-gel-derived organic-inorganic MIPs utilizes acid- or base-catalysed condition to achieve hydrolysis and condensation of numerous silane monomers.[15]   The compositions of sol and processing conditions including nature of solvent, pH, water/Si ratios, and type of catalyst play a significant role during imprinting of molecules in sol-gel-derived MIPs.[18]   Wei et al. have demonstrated that there is no significant adsorption toward caffeine when water/TEOS is equal to 2 due to TEOS is insufficient for hydrolysis.   The highest selectivity factor was occurred at water/TEOS of 5.[19]   Li et al. reported that the silica prepared at pH=2 possessed low re-adsorption capacities for bovine serum albumin because of inefficient template imprinting.[20]   However, the preparation of E2-imprinted organic-inorganic MIPs still receives less attention so far.   The present study focuses on preparation of E2-imprinted hybrid materials using a sol-gel synthesis route. Moreover, the selective adsorption of the imprinted organic-inorganic material toward E2 was demonstrated.
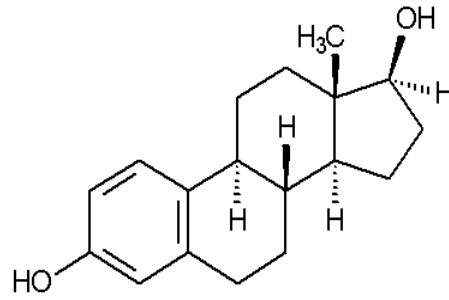
Figure 1- 1. The chemical structure of 17β-estradiol (E2).

1-2 Objectives

The aim of this study is to fabricate molecularly imprinted organic-inorganic polymers for recognition of E2 via a sol-gel method (Figure 1-2). The compositions of E2-imprinted polymers (porogen types, functional monomers test, cross-linker ratios, and TEOS/MTMOS ratios) and sol-gel parameters (catalysts, water/Si ratios, and pH values) are optimized to achieve the highest affinity. To elucidate the imprinted effect of the E2-imprinted polymers, the samples were characterized by BET and FTIR. Moreover, the sensitivity and selectivity of imprinted materials with E2 will be demonstrated.
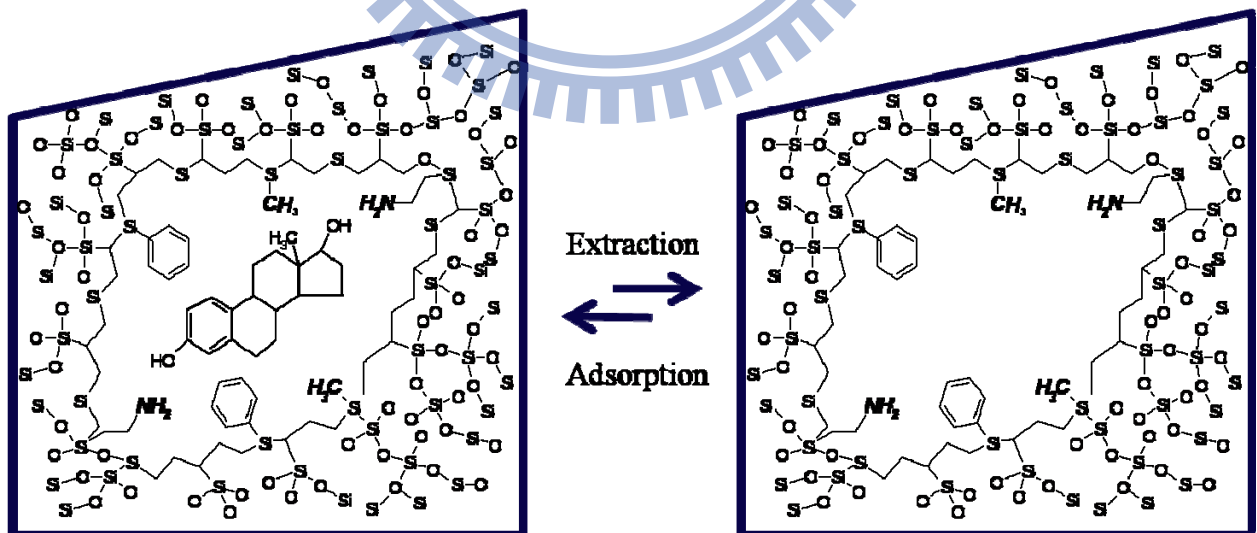
Figure 1- 2. The scheme of E2-imprinted materials.

3

Chapter 2.   Background and theory

2-1   Endocrine disrupted chemicals

2-1-1   Introduction

Recently, scientists have found that emerging environmental contaminant have high potential to cause disruption of endocrine systems and affect the metabolism and abnormal sexual development in aquatic organisms or wild life in very small concentration.   Those were called endocrine disrupting chemicals (EDCs).   Actually, the Organization of Economic and Cooperate Development define EDCs as ″an exogenous substance or mixture that alters the function(s) of the endocrine systems and consequently causes adverse health effect in an intact organism, or its progeny or (sub) pollution″.[21]   EDCs also called environmental hormones and wide variety of chemical compounds have been found to be capable of disrupting the normal endocrine functions.   Table 2-1 shows the list of EDCs including pesticides, surfactants, dioxins, polycyclic aromatic hydrocarbons, synthetic and natural hormones, and heavy metal.

EDCs are toxic and carcinogenic, and exist in the environment for a long time by their stability and bioaccumulation.   The effects associated with the presence of EDCs in the environment are: (1) feminization of male fishes, (2) toxic to the reproductive system and development in mammals, fishes, and birds, (3) eggshell thinning in birds of prey, and (4) causing irreversible damage to the aquatic life.   Moreover, the EDCs can lead some adverse effects in human health and the function of the endocrine system by binding to nuclear receptor.   The effects of EDCs in human beings reported so far have been (1) low sperm counts, (2) increase of the incidence of breast, testicular and prostate cancers, (3) early puberty, (4) carcinogenic and impotence at low levels, and (5) the endometriosis.[7, 21] Therefore, EDCs are great concern because of their potential in altering the normal endocrine

function and physiological status of organism.

Table 2- 1. List of some chemical compounds assorted as EDCs.[21]

No.	EDC class	Compound detected	Use/origin
1.	Phthalates	Butylbenzylphthalate, di-(2-ethylhexyl)phthalate and di-*n*-butylphthalate	They are found in detergents, resins, some addictives and monomers used in the production of plastics
2.	Pesticides	Dichlorodiphenyltrichloroethane, deltamethrin, carbofuran, atrazine, vinclozolin, carbendazim and tributylin	Extensively used in agriculture, insecticides, herbicides and fungicides are included in this class
3.	Organotin compounds	Tributyltin and triphenyltin	Compounds used in antifouling paints on ships
4.	Alkylphenols (surfactants)	Nonylphenol, etoxylate, octylphenol, octylphenol etoxylate	They are used during the production of phenol resins, plastic additives, and emulsifiers in agricultural or industrial applications
5.	Dioxins and furans	Dibenzo-*p*-dioxin, 2,3,7,8-tetrachlorodibenzo-p-dioxin , 2,3,7,8-tetrachlorodibenzofuran	They can be produced during the incineration of chlorinated aromatic compounds, paper and in the production of PVC plastic

No.	EDC class	Compound detected	Use/origin
6.	Bisphenols	Bisphenol A	It is used in the manufacture of polymers, flame retardants and rubber chemicals
7.	Parabens	Methyl, ethyl, propyl and butylparabens	Compounds used as preservatives in most cosmetics, personal care products
8.	Polychlorinated biphenyls	2,2′,4,4′-Tetrabrominated diphenyl ether, 2,5-dichloro-4,hydroxybiphenyl	Polychlorinated biphenyls have been used as coolants and lubricants in transformers, capacitors, and other electrical equipment. Although they are no longer being used, they are present in some old installation
9.	Polycyclic aromatic hydrocarbons	Fluorene, phenanthrene, fluoranthene, anthracene, pyrene, and naphthalene	Compounds generated during incomplete combustion processes of coal, oil, and wood
10.	Brominated flame retardants	Hexabromocyclododecane, poly-brominated diphenyl ethers and tetrabromobisphenol A	Compounds used in many products including furniture, textiles, electronic equipment
11.	Pharmaceuticals (synthetic steroids)	Diethylstilbestrol and 17α-ethinylestradiol	Pharmaceuticals mainly consists of oral contraceptives as well as steroids used for substitution therapy during menopause

No.	EDC class	Compound detected	Use/origin
12.	Phytoestrogens	Daidzen and genistein, matairesol, enterodiol and enterolactone	Natural substances found in many food plants such as grains, cereals, vegetables, fruits and others
13.	Natural hormones	Estrone, 17β-estradiol, oestriol	Estrogens naturally and daily excreted in the human urine and animals
14.	Heavy metals	Cadmium, mercury and lead	Industrial mining and metallurgy

2-1-2 Natural hormones

Among the various EDCs, natural and synthetic hormones are more interesting due to their high estrogenic potency. The natural hormones of EDCs produced by animal's endocrine system have frequently found in wastewater effluents and rivers.[22] Generally, estrone, estradiol, and oestriol are crucial natural hormones, since they are synthesized and excreted by the ovary every day. Upon entering human body, they can be toxic and carcinogenic even at trace concentration levels, and cause harmful effects such as inhibition of egg implantation and impotence.[1, 2] For example, the feminization of male fish occurs when reached E2 at 1-10 ng/L.[3]

2-1-2 Analytical methods

The most commonly used methods for E2 determination were including immune technique and instrumental analysis. Immunoassay assay including enzyme-linked immunosorbent assay and radioimmunoassay can be employed for multianalyte screening of a series of analytes because of ease use, relatively simple process, and fairly good sensitivity.[12] However, biological test systems also have limits to toxic environmental

contaminants or low stability in hash environment. The analytical instrument such as high-performance liquid chromatography and gas chromatography coupled with mass spectrometry and optical detectors currently have a good sensitivity and the ability to evaluate many pollutants in complicated mixture.   Nevertheless, they are costly investment, fussy procedure, and use of large amounts of organic solvents and environmental samples.[3, 6, 7]   The commercial column for analysis is expensive and less specific.

2-2   General strategy of molecularly imprinted method

2-2-1   Concept

Molecular imprinted polymers (MIPs) remained a potential method for the design and development of new materials with improved molecular recognition capabilities have been realized in recent years.[23]   The first concept of MIPs method is considered as the "lock-and-key" analogy with the action of a substrate and an enzyme, which proposed by Fischer in 1984.   The complementary to the shape of the substrate was imprinted by the enzyme′s active site, so that the substrate fits like a key into the specific lock of the enzyme. Following the concept, the molecularly imprinted polymer retains a "molecular memory" of template.   We named it ″molecularly imprinted polymers″ similar with lock and key.[24, 25]

Figure 2-1 shows the schematic representation of the molecular imprinting procedure. First of all, the functional monomers, template, and cross-linker will self-assembly.   Then, a pre-polymerization process with all species will spontaneously occur when the initiator present.   Subsequent polymerization, the functional monomers-template complexes are held in position by the formation of a rigid polymeric matrix.   Finally, removal of template using solvent extraction or combustion, the materials will be leaving a complementary cavity with the recognition ability in material.[26]   Therefore, the imprinting protocol yields a bulk material with specific recognition site for many applications.
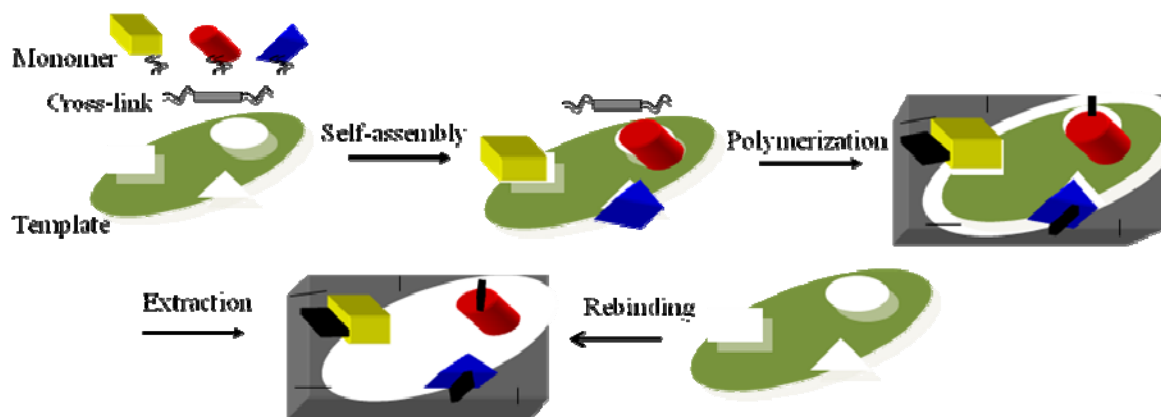
Figure 2- 1. Illustration of molecular imprinting process.

Synthetic polymer with molecular imprinting process is a protocol which based on the polymerization process in the presence of the imprint molecule, sometimes used target analyte or a molecule closely related to the target analyte. The cleavage of template creates the specific binding sites, which determining the selectivity and sensitivity. Actually, the created binding sites in MIPs can be classified into different types (Figure 2-2). Site A and Site B were expected specific recognition sites in MIPs. Virtually, site A with meso- and macro-pores (> 20 Å) is more accessible by analyte compared to site B with the smaller micro-pores (< 20 Å) where the mass transfer is slow. So, the porosity and large specific surface areas with accessible meso- and macro-pores are favored for transporting and diffusion in MIPs. However, some unfavorable conditions emerge in the final materials including inaccessible site (site C) and numbers of non-specific binding sites (site F). Their show low selectivity and sensitivity due to lack of specific cavities. In addition, template self-association is appeared (site D), if adding excess of template in preparation process, which also reduced the selectivity. Another unexpected types in MIPs are number of templates remained in materials after extraction process (site G) and induced binding site without deep cavity (site E).[27] Therefore, the cavities of MIPs have great influence on selectivity.

- **Site A.** In macropores
- **Site B.** In micropores
- **Site C.** Embedded
- **Site D.** Site coalescence.
- **Site E.** Induced binding site.
- **Site F.** Nonspecific site.
- **Site G.** Residual template
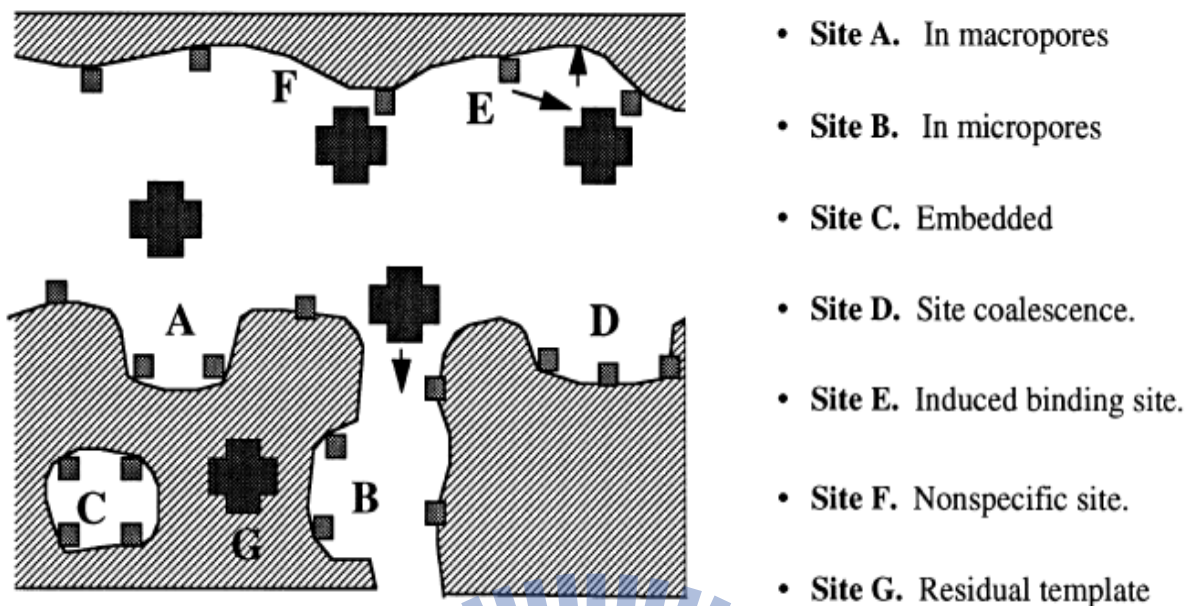
Figure 2- 2. Types of binding site in MIPs.[27]

2-2-2 Imprinting methods

Essentially, there are two imprinting methodologies to fabricate the MIPs. The methods of imprinting are according to interactions between functional monomers and template complex. Generally, the imprinting methods divide into two types including covalent and non-covalent interaction. Figure 2-3 displays the ordinary preparation of the covalent and non-covalent imprinting process.[26] Two of the procedures will facilitate produce the high network imprinted polymers which are rigidity and insoluble.
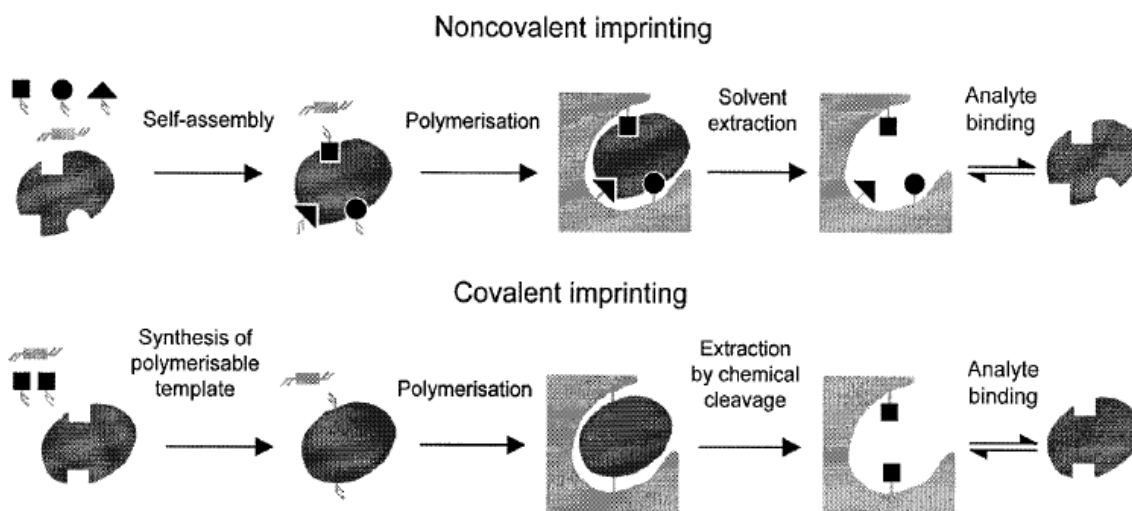
Figure 2- 3. The representation of the covalent and non-covalent imprinting process.[26]

The classical methods of covalent imprinting were approached via covalent binding such as boronic acid, diol, aldehyde, or amino groups within/inside cavity before the pre-polymerization.[25]   The functional monomers residues are only appeared in binding site, which may reduce non-specific interactions and degree of heterogeneity.[28, 29]   Although the stronger covalent binding is facile to generate the rigidity and homogeneity of binding site matrix, the subsequent extraction of template is more difficult to reach.[26]

In the simpler non-covalent imprinting, the interactions between template and functional monomers uses weak and easily reversible non-covalent bonds including hydrogen bond, electrostatic attraction, hydrophobic interaction, and electrostatic interaction.   Unlike those used in covalent imprinting, the fragile interaction is facilitated extraction or elution in the following procedure and easily obtained.   In addition, it generally offers much more variety of functionality in MIPs binding site.   However, the low yield of functional high-affinity receptor site and non-specific single point interaction were undesirable conditions for applications.[29]   The comparison of covalent and non-covalent imprinting process lists in Table 2-2.

11

Table 2- 2. The comparison of the covalent and non-covalent imprinting.

Terms	Covalent	Non-covalent
Pre-polymerization	Need for some degree of synthetic chemistry	No need
Extraction	Hard to remove the template	Easy to remove the template
Rebinding rate	Slow kinetic	Fast kinetic
Binding sites	Homogeneous of receptor sites	Heterogeneous of receptor sites
Advantages	1. Stoichiometric nature help to lower non-specific interaction. 2. High affinity receptor sites are easy produced.	1. The wide range of functional groups can be targeted. 2. Simplicity of the preparation process.
Disadvantages	1. More complex process. 2. A few types of functional groups can be used. 3. Lower template recovery.	1. Apparent non-specific binding. 2. Low yield of functional high-affinity receptor sites.

2-2-3 Synthesis

Different applications of the MIPs depended on their properties. The properties including format types, particle size, and samples required particular characteristic varied with different synthesis methods. So far, variety procedures for MIPs preparation have been developed. Organic-MIPs often formed by (1) bulk polymerization, (2) suspension polymerization, (3) precipitation polymerization, and (4) emulsion core-shell polymerization. The other method for inorganic or organic-inorganic hybrid MIPs is sol-gel method.

The bulk polymerization is first method to synthesis organic MIPs and vast employed due to the simplicity and university. First, template and functional groups dissolve in

adequate solvent. Then, template-functional monomers complex will present by covalent or non-covalent interaction when self-assemblely occurred. After cross-linker and initiator added, the above mixture solution underwent irradiation or heat derived to polymerize bulk monolithic format. The network of MIPs produced by cross-linker will preserve the template-functional monomers complex. Following, the template extracted by suitable extraction apparatus. In the end, they pulverized with a mortar and pestle for following sieve, and then preparation process finished. On the other hand, the solvent is used to create porosity polymers. The whole process involves some problems. There is represent less than 50% of the content loss in polymers during the serious of synthesizing imprinted polymers.[30] In addition, irregular particle created by grinding cause liable problem when packed into a column or coating the surface of transducer. On the other hand, the heterogeneity is produced under lack of control polymerization.

Another means for preparing MIPs is suspension polymerization. The suspension polymerization is occurred in organic solvent. The feature of the method is the surfactant involved the polymerization process to disperse unique particle which considered tiny bulk polymerization. Regarding precipitation polymerization, the mechanism is similar with suspension polymerization without surfactants. The precipitation of polymeric chain in the form of particles is based on the phase separation of solvent because they growth more and more insoluble in medium. The particle size in precipitation polymerization is around submicron (0.3-10 μm). There is no need stabilizer in this case because the rigidity obtained from cross-linker. This approach yields uniform size particles and the morphology is easily controlled. The core-shell particles are obtained by two steps process. The first step is emulsion polymerization. Seed latex can be prepared in this step. The second step is mixed with other monomers before the polymerization. The size, morphology, chemical properties can easy control in this method.[31] The other method for inorganic or organic-inorganic hybrid MIPs will discuss on next following section.

2-3-4　Template

One of the many attractive features of the molecular imprinted protocol is wide variety of print molecule which had successfully been used in recent year.　The imprinted of small organic molecules (e.g., amino acid, glucose, insecticides, nicotine, proteins and steroids) have successfully established for the preparation of selective recognition network, but the larger molecule structure employed in imprinted method is still a challenge.[26, 30]　A larger molecules is obstacle to the imprinted process and do not liable to create well-defined binding cavities.　Furthermore, the structure of larger molecule do not easy penetrate the matrix for reoccupation of binding sites.[30]　In the ideal polymerization with compatibility, templates choose must be chemically inert in preparation process.　Thus, the alternative imprinted process may be adjusted if the template will participate or unstable under polymerization conditions (e.g. elevated temperature for free radical polymerization or UV irradiation).[32]

2-3-5　Functional monomers

A functional monomer with functional groups plays an important role for producing a recognize site by formation of covalent or non-covalent interactions with the template.[6]　The functional monomers-template complex has to preserve in the polymerization process, and make sure of the functional monomers participates in formation of network.　In that way, the complex can be fixed in matrix.　Since the desirable template-functional monomers interactions (covalent and non-covalent bonds) were created in recognition sites, it is very helpful to define the applicable and congruous functionality monomers for the template and cross-linkers.[29]　Subsequently, removal of the imprint molecule leads to the cavities with matching size and shape to the analyte in polymers.　Therefore, the polymer rebinding the target analyte is high selectivity and sensitivity through complementary shape and size to the initial template.　In rebinding process, functional groups within the cavities will generate covalent and non-covalent interactions to analyte.　Therefore, the functional monomers not

only favor generation of cavities but also benefit to rebinding. The functional monomers normally are used in excess relative to the moles of template, and excess are preferring to non-specific binding.[32]

Typical functional monomers used carboxylic acids, sulphonic acids, and amino acids for non-covalent interactions; boronate ester, ketone, and aldehyde for covalent interactions; an iminodiacetic acid is commonly used for metal chelating interaction; and silanes are used in polysiloxane-based strategy. The majority of organic MIPs are based on both of functional groups of acrylate or vinyl monomers. In organic MIPs system, methacrylic acid is widely used function monomers due to the facile form of hydrogen bonds with variety target molecules. Generally, evaluation of the binding properties exhibits that hydrogen binding does certainty an important role in the molecular recognition in popular acrylic-based polymers during rebinding the target molecule. Figure 2-4 reveals some common functional groups for non-covalent and covalent MIPs.
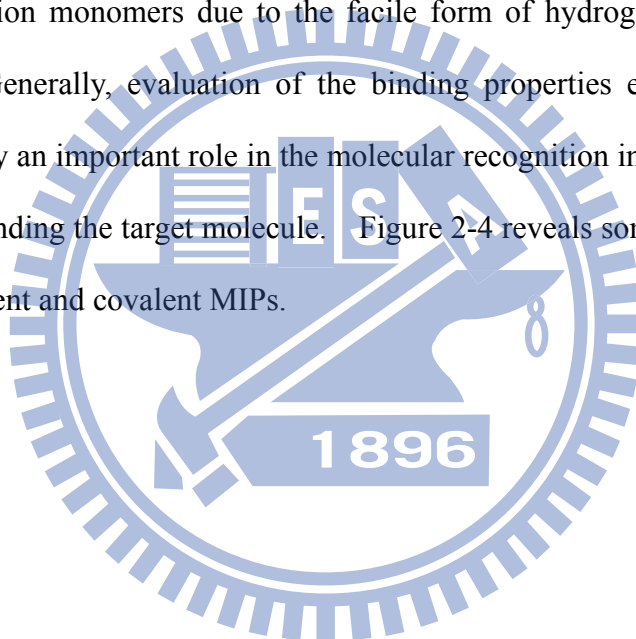
(a)
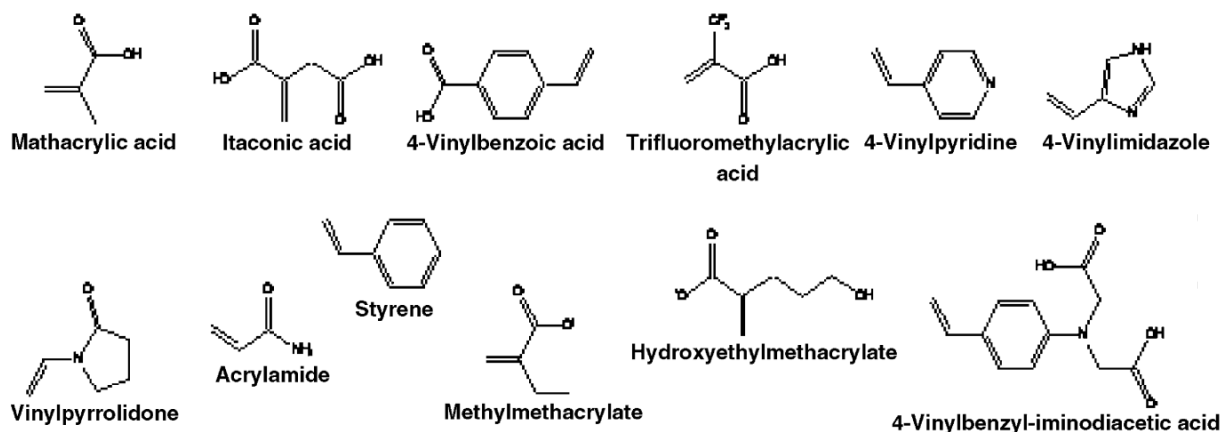
(b)
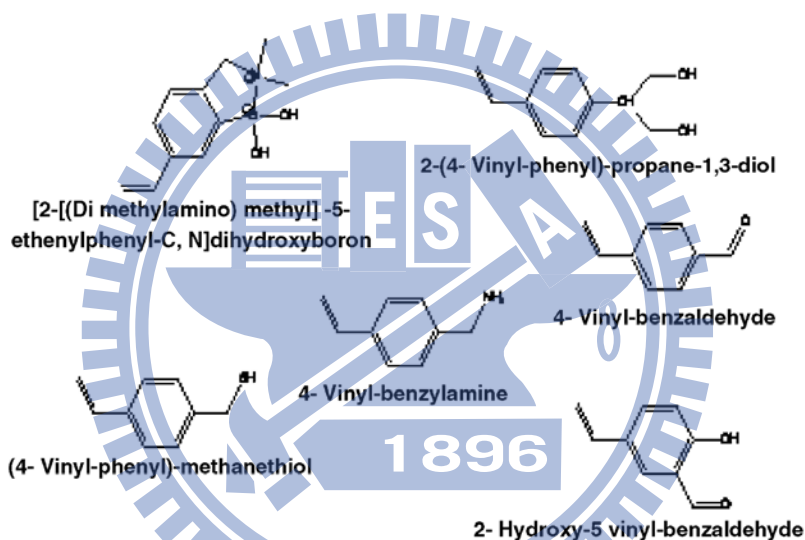
Figure 2- 4. Various functional monomers commonly used for non-covalent molecular imprinting (a) and for covalent molecular imprinting (b).[25]

2-3-6   Cross-linkers

In final imprinted polymers, the very high degree (70-98%) cross-linkers are necessary for fulfilling three dimensional structures.   Therefore, the cross-linkers of imprinted polymers provide materials some features.   First of all, the cross-linker is controlling the morphology and porosity of material matrix.   It is determining the diffusion of analyte into materials.   Secondly, it serves to fix the recognition site in network and stabilizes.   Finally, it participates in adequate mechanical stability of network.[32]   Owing to the formation of

network which is high polymeric nature via cross-link, MIPs with innately stable and robustness have been capable of chemical and thermal stable in hash environment.   Besides, it is notable the interaction of cross-linkers and functional monomers should ensure smooth incorporation in polymerization.   Appropriate ratios of cross-linker and functional monomers are crucial for maintaining recognitions specificity of a material.   The less level of cross-linkers induce the lower binding specificity, due to the functional groups are not sufficiently fixed by cross-linkers.   Conversely, the high levels cross-linkers reduce the loading capacity, and the extraction of template may also be hindered.[10]

Generally, divinylbenzene is used as cross-linker of styrene or acrylic-based MIPs and pentaerythritol triacrylate or pentaerythritol tetraacrylate is used for peptide-based MIPs. The other common crossl-inkers such as ethylene glycol dimethacrylate and trimethylolpropane trimethacrylate are utilized in many imprinting process.[32]   The chemical structure of various well-known cross-links commonly used for molecularly imprinted are shown in Figure 2-5.
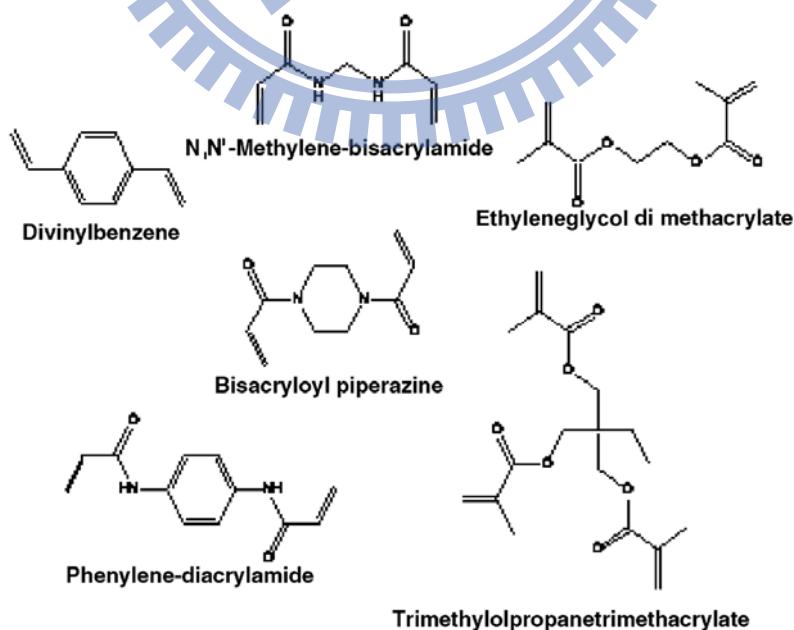
Figure 2- 5. Cross-linked monomers used to synthesis MIPs.[25]

17

2-3-7   Porogens

The solvent, referred to as porogen, used in the imprinting step is required not only to bring all the components in the polymerization but also responsible to generate a highly porous structure that raising the efficacious extraction and rebinding.[26]   The porosity of materials was determined by the type of solvent in the polymerization.   The phase separation between the growth polymers and solvent enhances the porosity structure.[33] Phase separate later occurred in higher solubility porogen in the polymerization will tend to produce small pore and higher specific surface areas of materials.   In addition, porogen with lower solubility induced phase separate early, which provides more large pore and lower specific surface areas of materials.[32]   Increasing the porogens content in the polymerization increases the pore volume of materials.   Beside, the use of more polar solvents such as acetic acid or methanol will tend to dissociate the molecule interaction such as hydrogen bonding or bridging of ionic salt between template and monomers, and imprinting is less sfficient.[10]   So, low solvent polarity including chloroform and benzene is desirable when the template and functional monomers interaction employed by non-covalent interaction.[30]

2-3   The inorganic - MIPs

2-3-1   Sol-gel process

The sol-gel process is a convenient and versatile method of preparing transparent optical glass or other ceramic material at ambient environment.   It is also enabling entrapment of numerous organic, organometallic and biological molecules within network by sol-gel derived process in laboratory.   In general, sol-gel materials have several advantages for example (a) compatible with organic and inorganic reagents, (b) physical chemical and thermal stable relates to organic polymers, (c) optically transparent and suitable for spectroscopic measurement.[18]   In addition, sol-gel process is facile to produce in a wide variety of forms: spherical shaped powder, thin film coating, inorganic membrane, or

extremely porous aerogel materials.   The schematic of sol-gel process and various products is shown in Figure 2-6.
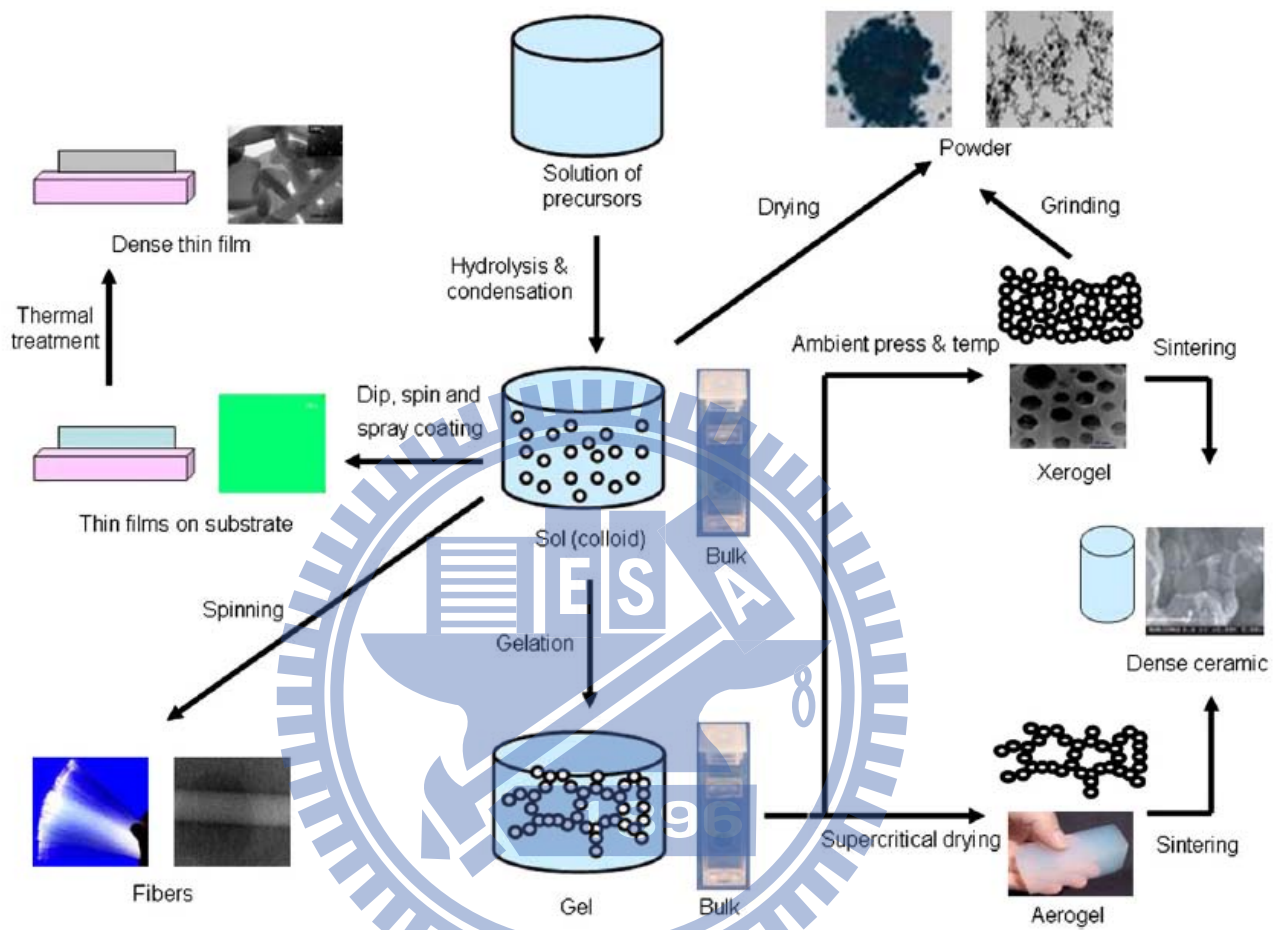
Figure 2- 6. The schematic of sol-gel process and various products.[18]

The basic sol-gel reaction involving three steps: hydrolysis, condensation, and polymerizations.   Figure 2-7 illustrates typical sol-gel process including hydrolysis, condensation and polymerization toward silica.   In practice, three of processes illustrate the aggregation process from colloidal suspension solution (sol) to gel phase.   They are included hydrolysis of precursors, condensation between hydroxyl groups, and finally gelation to gel phase when the metal alkoxide is mixed with water and a mutual solvent in presence of acid or base catalyst.[18, 25]

$$Si(OR)_4 + 4H_2O \underset{\text{Acid/base catalyst}}{\overset{\text{H}_2\text{O, Solvent}}{\rightleftharpoons}} Si(OH)_4 + 4ROH$$

$$\equiv Si-OR + HO-Si\equiv \underset{\text{Alcoholysis}}{\overset{\text{Aldol Condensation}}{\rightleftharpoons}} \equiv Si-O-Si\equiv + ROH$$

$$\equiv Si-OH + HO-Si\equiv \underset{\text{Hydrolysis}}{\overset{\text{Water Condensation}}{\rightleftharpoons}} \equiv Si-O-Si\equiv + HOH$$

$$\left[\equiv Si-O-Si\equiv\right]_n \overset{\text{Polymerization}}{\longrightarrow} \text{Silica polymeric matrix}$$

Figure 2- 7. Typical chemical reaction in sol-gel process toward silica.[18]

In hydrolysis step, the precursor hydrolysis with water results hydroxylated products and corresponding byproducts (alcohol or water). Following step is condensation between an alkoxide groups and a silane groups or two silane groups yield siloxan and byproduct of alcohol or water, respectively.[25] These constituents further continue to hydrolyze and condense, and forming sol solution (colloidal suspension of very small particle, 1 to 100 nm). It can cast into files, powders, and fibers at the moment. Generally, both hydrolysis and condensation reactions in sol-gel process occur simultaneously while the hydrolysis reaction has been intiated.[18] In the polymerization step, the condensation between sol particles becomes rigid, nano-porous, three-dimensional network of gel. During drying process, the solvent, or residue alcohol and water will evaporate from the pores or network and increase the strength of the sol-gel processed materials. It may causes substantial shrinkage and cracking, leading to the various degrees of the morphology changed. On the other hand, the

chemical or physical properties of the materials are attributed by controlling environmental parameter such as pH value, chemical reaction of the three processes, content of water, and surrounding temperature.

The sol-gel reaction mechanism in acid or base catalyzed system is mainly initiated from electrophilic and nucleophilic attachment. In acidic condition, the alkoxysilanes were hydrolysis through the fast protonation of a leaving alkoxy group, and subsequent nucleophilic attack of water forms the five-coordinate transition state.[34] Partial positive on alkoxide would raise the rate of hydrolysis by providing electrons and reduce the rate of condensation by steric effect, leading smaller particle and average pore size. The final linear and non-shaped product is yielded from acid-catalyzed and base-catalyzed route, respectively.

Another non-hydrolytic sol-gel method also has been recognized as a versatile route of synthesizing silica, titania, alumina, inorganic oxides and mixed or binary oxides in a facile process, which can be carried out in the absence of any solvent. In its general form of NHSG process comprehend the reaction of a metal halide with an oxygen donor such as an alkoxyde, or an alcohol, and leading to the formation of inorganic oxides under solvent-free condition.

Alcoholysis

Condensation
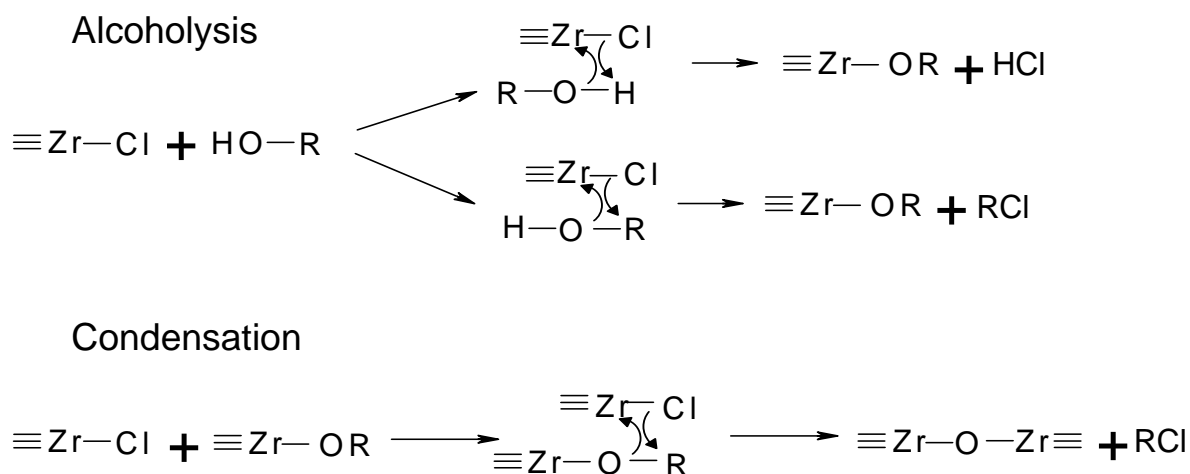
Figure 2- 8. Non-hydrolytic sol-gel route to inorganic oxides.

To illustrate the mechanism of non-hydrolytic sol-gel, the Figure 2-8 showed the NHSG typical reaction to inorganic oxides. The non-hydrolytic sol-gel mechanism reaction involves a lone pair of electrons of an alcoholic oxygen atom to the central zirconium atom of halide, followed by the cleavage of either the hydroxyl or alkoxyl group. The occurrence of ligand exchange reaction via intermediate Lewis adducts can change the mechanistic and kinetics route of the reaction as well as redistribution of the product in NHSG process. Accordingly, the byproduct of this procedure is commonly an alkyl halide whose formula depends on the utilization of different of oxygen donor molecule. The zirconium metal in Figure 2-8 can be exchanged to silicon, titanium, or aluminum and catalyzed via Lewis acid with the common iron (III) chloride.

2-3-2 Merits of Sol-gel process in molecular imprinting

The preparation of sol-gel imprinted materials were inorganic based polymers under acid or base catalyzed hydrolysis and condensation process in present of precursor and template. The first approach to construct inorganic MIPs was traced back to early 1930s. Chronologically, the development of inorganic MIPs is shown in Table 2-3. The imprinted

sol-gel materials have been produced and applied as adsorbents, sensing materials, separation

media, catalysts and sensing phases.

Table 2- 3. The development of inorganic MIPs.[35-37]

Yeas	Contents
1931	Poljakov removed water from a silica gel in an atmosphere of benzene, toluene or xylene, and found that the pore structure was influenced by the size and shape of the molecules in the gas atmosphere.
1942	Pauling and Campbell reported the preparation of artificial antibodies using antigen molecules as templates.
1949	Dickey prepared imprinted gels from acidified silica solutions in the presence of methyl orange, after extraction, adsorbed methyl orange better than a blank gel.
1952	Curti et al. expanded the concept of Dickey to the separation of enantiomers by imprinting silica with an enantiomer.
1960s	Klabunovskii et al. further expanded the concept of molecular recognition to the resolution of racemic mixtures.
1972	Wulff and Sarhan elucidated that the selectivity of imprinted polymers depend not only complementary cavities but also orientation of functional monomers within cavities.
1985	Mosbach et al. allowed organic silanes to polymerize on the surface of porous silica particles in aqueous solution and obtained superior support by imprinted dye molecule.
1998	Lee et al. developed the molecular imprinting of azobenzene carboxylic acid on a TiO_2 ultrathin film by the surface sol-gel process
2008	Hu et al. combined colloidal crystal and molecular imprinting for theophylline sensing.

The traditional methods for preparing organic MIPs may shrink or swell when exposed to different mobile phase, and they may change the morphology of organic MIPs and the essential for recognition.[1]   Relating to organic MIPs, sol-gel process affords some advantages for preparation of inorganic MIPs.   The advantages include mild condition permits the template that is water soluble,[28] gelation at ambient temperature (particularly important when preserving weak interaction), high porous structure, ease of preparation, good optical properties and good solvent resistance.[15]   Silica based materials are extremely rigid structure; the property has provided integrity cavity which created by the template removal. High thermal stability of sol-gel materials offers an alternative way to remove template by calcinations method.   In addition, sol-gel derived materials are structurally porous, and high specific surface areas can improve mass exchange.   Sol-gel method also provides an efficient route for generating hybrid matrix by incorporating organic component into inorganic network under mild condition.   On the other hand, the tunable sol-gel imprinted process can ease control physical and chemical propertied including pore size, porosity, surface functional and rigidity.[38]   The preparation of imprinted materials via sol-gel process can be approached in many formations of the products (see Figure 2-9).[17]

The non hydrolytic sol-gel methodology used to fabricate imprinted polymers has some advantages.   Due to the liquid phase displays the some drawbacks in the reaction, the non-hydrolytic sol-gel method offers the potential to avoid the use of solvent.   In this way, an attractive alternative to hydrolysis sol-gel route, non-hydrolytic sol-gel can fabricate monoliths that do not require aging and drying steps at high temperature.   Once the shrinkage and cracking were avoided, the loss of affinity of imprinted polymer was reduced. The NHSG imprinted materials also affords the elimination of residual silanol groups in the polymer, which reduces the non-specific interaction.[39]   In practice, they chose of experimental conditions in NHSG process have important implications for the mechanistic course when generating certain forms of hybrid.[40-42]
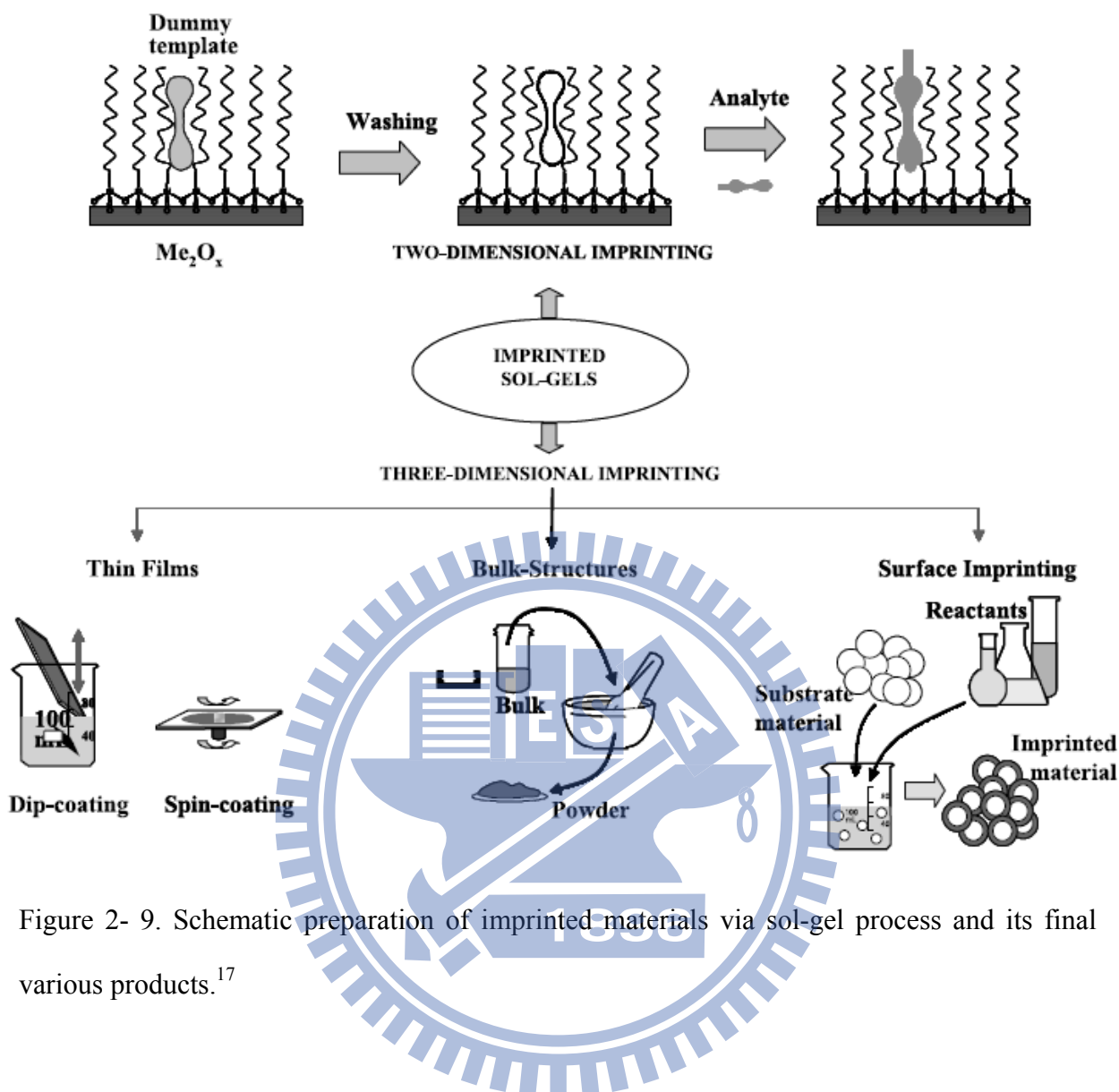
Figure 2- 9. Schematic preparation of imprinted materials via sol-gel process and its final various products.[17]

2-3-3 pH effect

The pH value has great inflecting on not only the morphology, particle size, and optical property but also reaction rate of the final products. In low pH condition, acid-catalyzed produces liner or randomly branched polymeric sol-gel network with small size particle; whereas in high pH condition, base-catalyzed hydrolysis produces more highly branched polymeric network with large particle due to the high solubility in base solution. In general, the hydrolysis rate is inverse proportion with increase pH value at pH<2 or pH>7, and direct proportion with increase pH value at 2<pH<7. The condensation rate also determines by the pH of sol-gel process and is highest at intermediate pH. At neutral condition, the gelation

25

time is short whereas at low pH, gelation time is very long.   Sometimes, gelation time is decreased by factors that increase in the temperature and concentrations of precursor and decrease in the size of alkoxy group and content of water.[18]   The refractive index and pore volume of materials are also determined by pH.   In addition, the specific surface areas and pore volume were larger when using ammonia hydroxide as the catalyst than was fund when using hydrochloric acid.   Either lower concentration of catalyst gave a porous network.   However, the formation of porous structure yields the non-specific binding.[43]

2-3-4   Water/siloxane

Water plays an important role in sol-gel process.   Generally, the amount of water will regulate the reaction rate in hydrolysis and condensation step.   The enhancement of the amount water increases the hydrolysis rate, but decreases the condensation rate due to the dilution of the concentrations of silane.   In high water content, the hydrolysis will complete, that helps more hydroxyl group condensation and causes large particle occurred.

2-3-5   Organic-inorganic hybrid MIPs

One of the major advances in sol-gel technique is the possibility of incorporating the specific organic group into inorganic matrix for improvement of sensitivity and selectivity. The combine the properties of organic and inorganic in one material called organic-inorganic materials or organically modified silanes.   Thus, the properties of organic-inorganic material were adjusted by varying the chemical composition and the ratio of precursor.   Table 2-4 lists some inorganic precursors and monomers for organically modified silanes.

Table 2- 4. Some inorganic precursors and monomers for organically modified silanes.

Inorganic precursors	Monomers	Ref.
Tetraethyl orthozirconate	Methyltrimethoxysilane Methyltriethoxysilane	18, 20, 44-50
Aluminium tert-butoxide Aluminium chloride	Phenyltrimethoxysilane Phenyltriethoxysilane	18, 23, 44-52
Tetraethyl-orthotitanate	3-(triethoxysilyl)propyl isocyanate 3-mercaptopropyltrimethoxysilane	1, 38, 43, 53-56
Tetramethyl-orthosilicate		
Tetraethyl-orthosilicate	3-aminopropyltrimethoxysilane 3-aminopropyltriethoxysilane	16, 20, 53-55, 57-61

27

The melding of MIPs technique with sol-gel method in the hydrophobic medium may stand for a novel synthetic strategy for the preparation of organic-inorganic hybrid MIPs.[62] The organic functional monomers can produce interaction to template and favor for generation of cavities within silica matrix. Hence, the selectivity and sensitivity can be achieved by organic-inorganic MIPs. The outstanding inorganic properties including chemical and thermal stability, high porous and mechanical strength were presented in organic-inorganic MIPs by sol–gel silica network. Therefore, the enhancement of stability in the polymer matrix to prevent the disruption or swelling and high porosity of the material may be attributed to the inorganic compound to hybrid MIPs composition.[63] On the other hand, the organic properties provide the hybrid MIPs materials more flexibility, low density, and specific binding ability. The stability and low fabrication cost makes these hybrid polymers adaptable for various applications.[64] On the other hand, the finding that TEOS is established to undergo spontaneous hydrolysis and condensation reactions in a prevalent formation of hybrid MIPs than organic MIPs process. Because of the formation of organic MIPs is utilizing hazardous organic solvent (chloroform or toluene) as porogen to preserve the ion and hydrogen interaction. However, the undesirable condition including chemical incompatibility and phase separation is a obstacle to form a true hybrid materials.[62]

2-4 Applications of MIPs

MIPs methods have been employed in analytical technique including membrane liquid-liquid extraction,[65] pharmaceutical separation,[39, 66] liquid chromatography,[5] clinical diagnostics, asymmetric catalysis,[11] food analysis, production monitoring,[7] solid phase extraction,[16, 38] and chemical sensor.[12, 24, 26, 62, 67, 68] Figure 2-10 displays the common MIPs put to use in analytical chemistry.
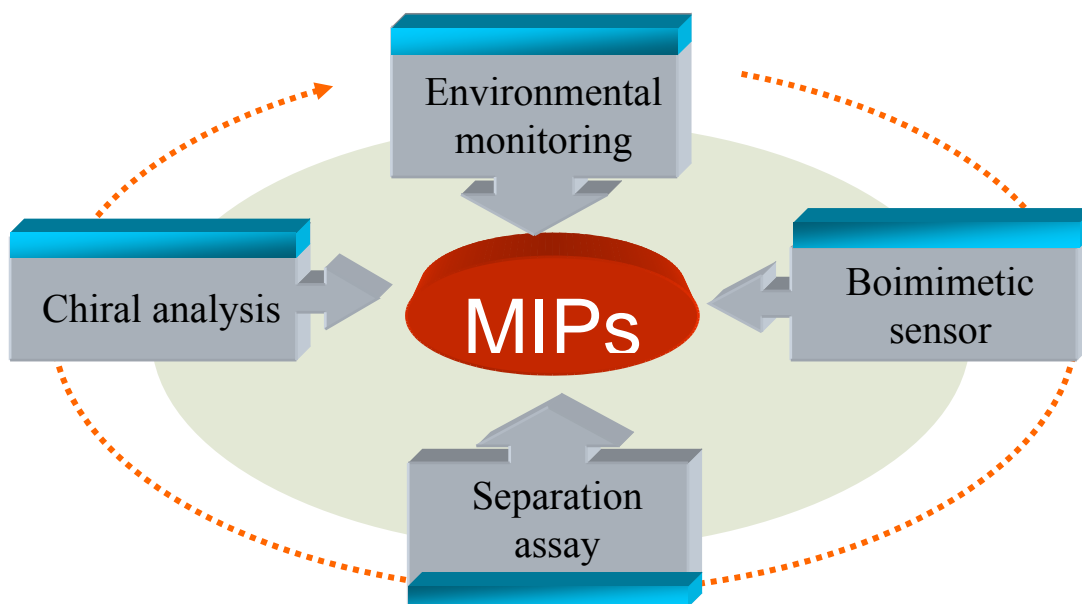
Figure 2- 10.   The applications of analytical chemistry.

2-4-1   Sensing materials

A chemical sensor used to detect the analyte is normally combines the central part of recognition element and a transducer.   The sensing elements are immobilization at the interface between the sensor and the analyte.   In typical sensing mechanism, sensing materials change their properties upon exposure of analytes and then transducer translate those chemical and physical properties into useful information to determine the composition or quantity of analytes.   Those change chemical and physical properties including conductivity, ampere, or impedance in electrical properties, absorbance or refractive of optical properties, gravimetric or viscoelastic detection in mechanical energy, or calorimetric or pyroelectric detection in thermal properties.[8]   The common sensing materials for chemistry analysis were metal oxides, metal complex, organic polymers, and carbon nanotube.

The semiconducting nature of metal oxides can employ to detect the surrounding changes with the electrical conductivity.   The metal oxide sensor is normal working at 200 ~ 500 $^{\circ}$C then some charged species such as O_2-, O-, and O2- are absorbed on the surface of

metal oxide.   In this condition, if a reduction of analyte is adsorbed on the materials, it will be oxidized and generates electrons, which increase the conductivity of the materials.   In addition, materials with higher area/volume ratios meliorate the sensitivity and response time because this favors adsorption of gases on materials.   The addition of transition metal ions in metal oxide also favors the sensitivity.   Because the more charged species adsorbed the more electrons in network, which can reduce the conductivity and increase the sensitivity.[69]   On the other hand, transition metals usually used to metal complexes due to the capable of generating reversible interaction to analytes.   Moreover, the coordination bonds are constructed between the materials and analytes in adsorption process and can be broken by change the chemical environment.   The advantages of employing metal complexes are designed to interact with a specific analyte, hence increasing the selectivity and reusable. The drawback of synthesizing the metal complexes is expensive.[69]

Sensors with organic polymer for humidity sensing have been developed.   The detection mechanism is that the protons of the amino group on polymer surface decreases upon contacting the atmosphere water and then H_3O+ was formed.   Following, the electrical conductivity of material will increase accompanied with increasing of the electron pairs for charge transport.   Organic polymers-based sensing materials are cheap and high sensitivity but lack of selectivity and lower chemical stability may be main problems.   Carbon nanotubes with high stiffness and strength can be metals or semiconductors, depending on its chirality.[70]   The considerable interest in changing conductivity of carbon nanotube in the presence of gases can be applied to design sensing materials.   The phenomenon is present when the analyte is an electron donor.   The number of holes on the nanotubes will decrease, leading to a decrease in electrical conductivity.   In contrast, if the analyte is an electron acceptor, electrical conductivity will increase.[69]   In addition, carbon nanotube has led to sensitive materials due to high area/volume ratios, which can easy react with analytes by increasing adsorption site.   The lack of selectivity for raw carbon nanotube is the

30

shortcoming.[69]   Table 2-5 summarizes the advantages and disadvantages of typical sensing

materials.

Table 2- 5. Main advantages and disadvantages of sensing materials.[69]

Material	Pros	Cons
Metal oxides	• Doping with metal increasing the sensitivity and selectivity.	• The complex preparation process. • Working at high temperature
Metal complexes	• The detection is based on specific reaction. Therefore, they possess selective in many case.	• Synthesizing the complex is expensive.
Organic Polymers	• With a thin polymer layer, response times are short and reproducibility is high.	• Stability and selectivity are low.
Carbon nanotubes	• Shorter response and recovery times. • Work at room temperature.	• Additional purification processes are required. • Lack selectivity for raw CNTs. • Relatively expensive.

The application of MIPs for the territory of analytical chemistry has been published in

many literatures.   An aspect in design of a MIPs-based sensor is somewhat important due to

the low price, chemical stabile and high selectivity.   Another obvious advantage of the

polymer is synthesized in situ at the transducer conducting surface such as gold or the surface

can be coated with a preformed polymer but requires specialized polymer recipe.[26]   In order

to synthesis the membrane for sensors, most application cases are employing standard surface

coating techniques such as spin coating, dip coating, and spray coating.   They have been

used to apply a formation of thin film layer to acoustic transducer surface or quartz crystal microbalance.[26, 71] Change physicochemical of system upon binding analyte are used for detection. Transducers employed in MIPs based sensor include fluorescence, or electrochemical methods (voltammetric, capacitance, amperometric, or conductometric methods), and mass-sensitive sensors.[26, 71] Table 2-6 summarizes the illustration of utilizing the transducer depend on the imprinted polymer based sensor.[26] The MIPs based electrochemical sensor is detection based on the change in electrochemical of device. In recent years, mass-sensitive acoustic transducer including surface-acoustic wave[72] and quartz crystal microbalance[24, 67, 68, 73-75] have been used to combine with MIPs. First of all, the MIPs film is coated on the SAM and QCM oscillators. The MIPs shows a selective adsorption toward target analyte. The change in oscillation frequency is resulting from the mass change at the oscillator surface and quantified by piezoelectric microgravimetry.[26] On the other hand, if the target species exhibits inherent chemical property such as optical and fluorecence, this can use transducers such as uv-visible and fluorescence for detection.

Table 2- 6. The transducer used for MIPs sensors.[26]

Transducer	Analyte	Useful range(μM)
Capacitance	Phenylalanine	Qualitative
Surface acoustic wave	Solvent vapors	0.1μL/L
Quartz crystal microbalance	S-propranolol	50-1300
Fluorenscence	Dansyl phenylalanine	25-250
Amperometry	Morphine	3.5-35
Voltammetry	2,4-dichlorophenoxyacetic acid	0.1-100

Molecular imprinted materials for gas phase sensing have been studied. Table 2-7 lists the application of MIPs-based materials for gas sensing in decade. The most used transducer of MIPs sensor for gas phase sensing is quartz crystal microbalance, owing to high sensitivity of quartz crystal microbalance. Combination of selectivity of coating MIPs

materials and sensitivity of transducer, it can be a sensor for vary of analytes.   The detection

limit of those sensors is achieved at low concentration; it is useful for many applications.

Table 2- 7. The applications of MIPs-based materials for gas sensing.

Template	Detection	Detection limits	Ref.
Parathion	Quartz crystal microbalance	1ppm	[71]
2-methylisoborneol	Quartz crystal microbalance	10 ppb	[74]
Formaldehyde	Quartz crystal microbalance	75-900 ppb	[67]
L-menthol	Quartz crystal microbalance	200 ppb	[66]
Toluene	Quartz crystal microbalance	540 ppm	[68]
Phenol	Quartz crystal microbalance	300 ppm	[39]
2,4,6-trinitrotoluene	Quartz crystal microbalance	300 ppm	[73]
Sarin acid	Surface acoustic wave	0.1 ppm	[72]

2-4-2   Separations

The separation abilities of molecularly imprinted polymers method are achieved in the

fields of an active pharmaceutical compound,[66] resolution of enantiomorph,[39] and solid phase

extraction.[16]   One of the close practical applications of MIPs is as sorbent for solid phase

extraction.   The typically sorbent for SPE such as inorganic oxides and silica have impure

extracts or low recoveries problems.   However, the facile, reproducibility, and specificity

advantages of MIPs-based solid phase extraction were an attractive application for

separations.[16, 30]

Chapter 3.   Materials and Methods

Figure 3-1 displays the flow chart of the experimental design for preparation of sol-gel-derived E2 imprinted silica in this research.   The preparation conditions including porogen, functional monomers, cross-linkers, TEOS/MTMOS, catalysts, pH values, and water/Si ratios were optimized to obtain the highest rebinding ability.   Moreover, the compositions and textures of the MIPs were characterized by gas adsorption, Fourier transform infrared spectrometer (FTIR), and thermogravimetric analysis (TGA) to elucidate the effect of imprinting cavities and functional monomers on the adsorption behaviors.   Finally, the adsorptions of analogues were examined to understand the recognition ability of MIPs toward to the target compound

3-1   Chemicals

All reagents used in this study were commercially available and were used without further purifications.   Tetraethyl orthosilane (TEOS, $(C_2H_5O)_4Si$, Fluka, 99%) was used as the precursor of silica and the cross-linker in sol-gel process.   3-aminopropyltriethoxysilane (APTES, $H_2N(CH_2)_3SiOC_2H_5)_3$, Sigma-Aldrich, 99%) and phenyltrimethoxysilane (PTMOS, $C_6H_5Si(OCH_3)_3$, Sigma-Aldrich, 97%) were used as the functional monomers which bound the target compound 17β-estradiol (E$_2$, $C_{18}H_{24}O_2$, Alfa Aesar, 97%) via hydrogen bond and π-π stacking interactions, respectively.   Methyltrimethoxysilane (MTMOS, $C_4H_{12}SiO_3$, Sigma-Aldrich, 98%) was employed to increase the hydrophobicity and flexibility of polymers.   Nonylphenol ($C_{15}H_{24}O$, Riedel-de Haën, 99.9%), 1-naphthaol ($C_{10}H_8O$, Riedel-de Haën, 99%), progesterone ($C_{21}H_{30}O_2$, TCI), and testosterone ($C_{19}H_{28}O_2$, TCI) were used in selective adsorptions.   Absolute ethanol (C_2H_5OH, Sigma-Aldrich, HPLC grade, 99.8%), acetonitrile (C_2H_3N, Echo, HPLC grade, 99.9%), tetrahydrofuran

(C_4H_8O, Mallinckrodt, HPLC grade, 99.9%) were employed as porogens. Hydrochloric acid (HCl, Hanawa, 35%) and acetic acid (HAc, $C_2H_4O_2$, Scharlau, 99.8%) were employed for catalysts test. In contrast to non-covalent bonding, 3-isocyanatopropyltriethoxysilane (ICPS, $C_{10}H_{21}NO_4Si$, Sigma-Aldrich, 95%) was used to prepare monomer-template complex (E2Si) with E2 via covalent bond using dibutyltin dilaurate (DBDU, $C_{32}H_{64}O_4Sn$, Sigma-Aldrich, 95%) as the catalyst. Dimethyl sulfoxide (DMSO, C_2H_6OS, Sigma-Aldrich, GC grade, 99.7%) was used as the extraction solvent for the covalent MIPs. Furthermore, toluene ($C_6H_5CH_3$, J.T. Baker, HPLC grade, 99.9%) and methyl alcohol (CH_3OH, Mallinckrodt, HPLC grade, 99.9%) were employed as adsorption solvent in this study. Deionized water (DI, Millipore, 18 MΩ cm) was obtained from Milli-Q water purification system used throughout the experiments. Table 3-1 shows the structures of the major reagents used in the imprinted polymers.
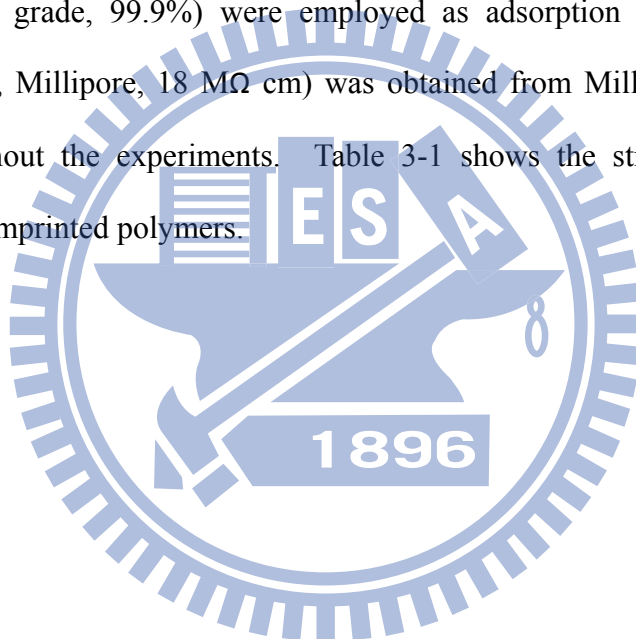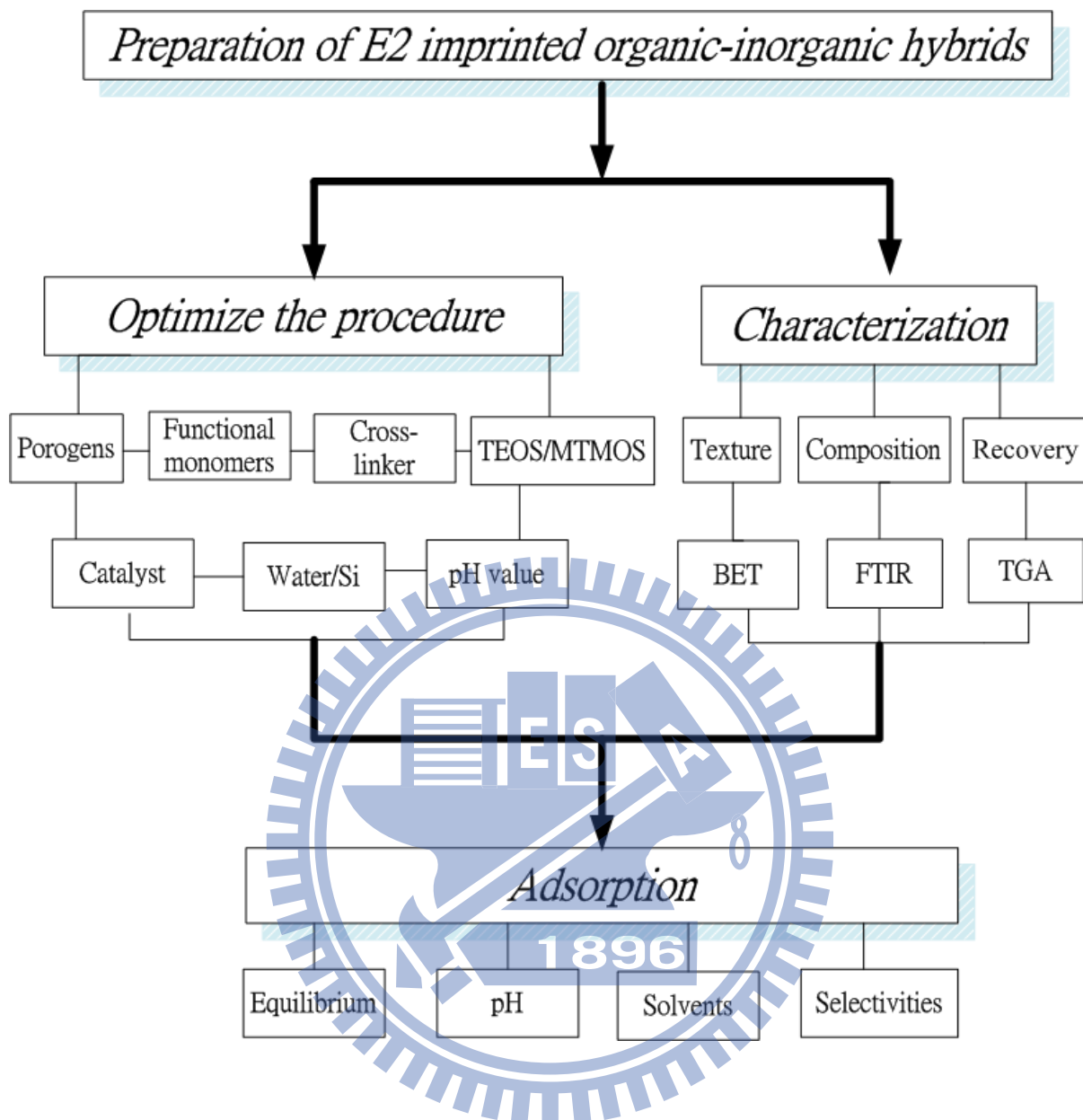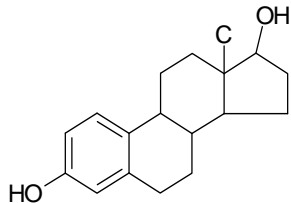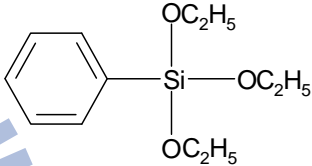
Figure 3- 1. Flow chart of experimental design in this study.

Table 3- 1. The structure of the major reagents used in imprinted polymers.

Reagents	Name	Abbr.	Structure
Template	17β-estradiol (Target compound)	E2	
Cross-linker	Tetraethylorthosilicate	TEOS	
Monomers	Phenyltrimethoxysilane (for non-covalent)	PTMOS	
	3-aminopropyltriethoxysilane (for non-covalent)	APTES	
	Methyltrimethoxysilane (for non-covalent)	MTMOS	
	3-isocyanatopropyltriethoxysilane (for covalent)	ICPS	

3-2 Sol-gel process to MIPs

3-2-1 Non-covalent MIPs

Molecularly imprinted organic-inorganic materials were produced by a sol-gel process. Figure 3-2 shows the preparation process of sol-gel-derived MIPs. A 2.26 mL of TEOS together with 0.145 mL of MTMOS, and 5 mL of ethanol were mixed thoroughly at 200 rpm

in a 20 mL sample vial at room temperature.   A 0.99 mL of DI and 0.12 mL HCl (0.1M) were added to the precursor solution slowly and mixed at room temperature for 30 min, then kept at 80 ^{o}C for 1.5 hr to hydrolyze and yield the sol.   The homogeneous solution contained 5 mL of ethanol, 0.18 mL of PTMOS, 0.24 mL of APTES, and 0.14 g of E2 at a molar ratio of TEOS:PTMOS:APTES:E2=20:2:2:2:1 were added into the above solution.   The mixture was stirred vigorously at 200 rpm at 80 ^{o}C for 2 hr.   Then, condensation reaction was processed in the open vial at 60 ^{o}C in oven for 48 hr until gelation.   The solution turned gradually from transparent to opaque white gel during the solvent evaporation.   When the synthesis was completed, the gel monolith was dried at 100 ^{o}C for 6 hr in oven to evaporate the residue water and solvent.   The gel was then crushed with a mortar and pestle into fine powders.   A non-imprinted gel (NIP) was prepared using the same procedures except the addition of template (E2).

The crushed powders were immersed in 40 mL of hot methanol at 85 ^{o}C for 4 hr under stirring to remove the template.   Washing was repeated 16 times until no trace of E2 could be detected.   Further, the powders were washed by 20 mL fresh acetonitrile for 2 times and were dried at 70 ^{o}C.
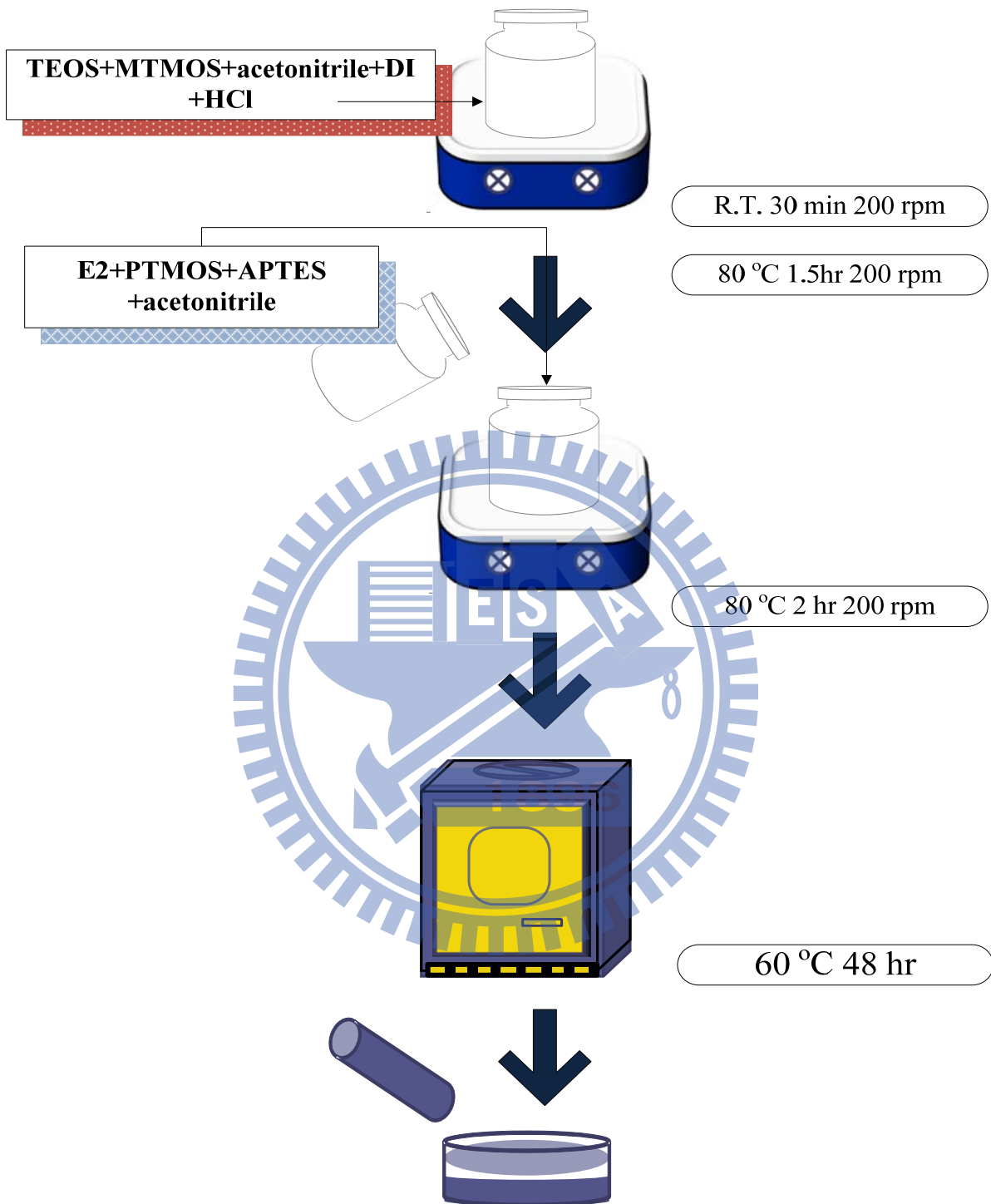
Figure 3- 2. Preparation process of molecular imprinted organic-inorganic materials for E2.

3-2-2　Covalent MIPs

For comparison, covalent MIPs were prepared using ICPS as the functional monomer. The ICPS was initially reacted with the phenol group of E2 to form urethane bond in the presence of DBDU.　Figure 3-3 shows the mechanism of the reaction.　A 0.14 g of E2 was dissolved in 5 mL of tetrahydrofuran with stirring at 200 rpm for 5 min.　Then, 0.262 mL of ICPS and 0.05 mL of DBDU were added slowly into the E2 solution and underwent the reaction at 100 $^{\circ}$C for 24 hr under nitrogen atmosphere.[43, 53-55]　The solution was called solution A.

On the other hand, 2.26 mL of TEOS, 0.145 mL of MTMOS, and 5 mL of tetrahydrofuran were mixed thoroughly at 200 rpm in a 20 mL sample vial at room temperature to form the precursor solution.　A 0.99 mL of DI and 0.12 mL HCl (0.1M) were added to the precursor solution slowly and mixed at room temperature for 30 min and then kept at 80 $^{\circ}$C for 1.5 hr to hydrolysis and yield the sol.　Afterwards, the solution A and 0.18 mL of PTMOS were added into above solution.　The mixture was stirred vigorously at 200 rpm at 80 $^{\circ}$C for 2 hr.　Then, condensation reaction was processed in the open vial at 60 $^{\circ}$C in oven for 48 hr till gelation.　When the synthesis was completed, the gel monolith was dried at 100 $^{\circ}$C for 6 hr and crushed with a mortar and pestle into fine powders.

The template was extracted from the silica matrix by heating in a DMSO/DI (100 mL/20mL) solution at 190 $^{\circ}$C for 8hr.[53, 54]　In the presence water, the isocyanato group was dissociated and converted to an amino group.　The extraction mechanism of covalent MIPs was showed in Figure 3-4.　Further, the powders were washed by 20 mL fresh aceonitrile for 2 times and were dried at 70 $^{\circ}$C.
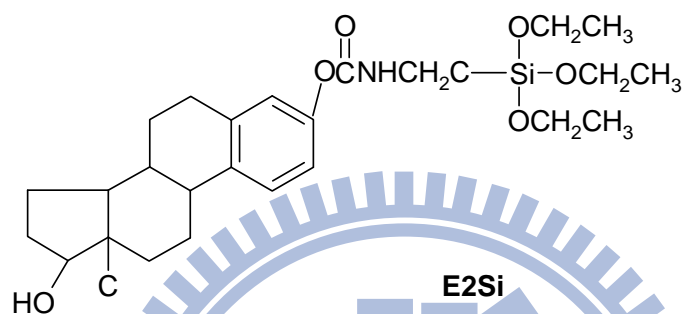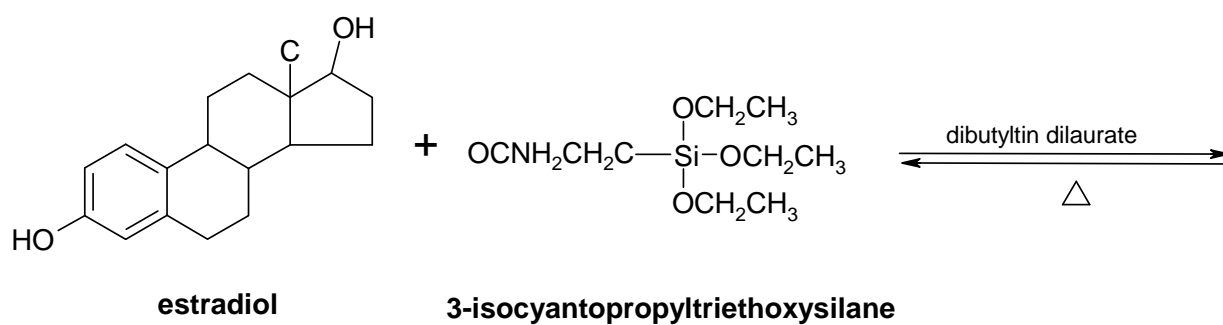
Figure 3- 3. Formation of urethane bond between E2 and ICPS.
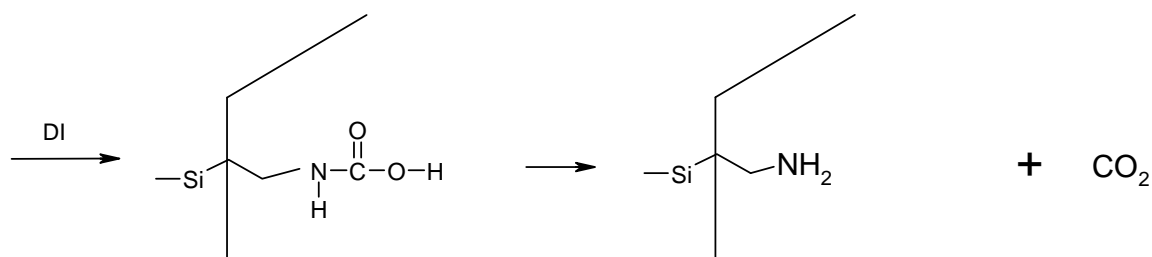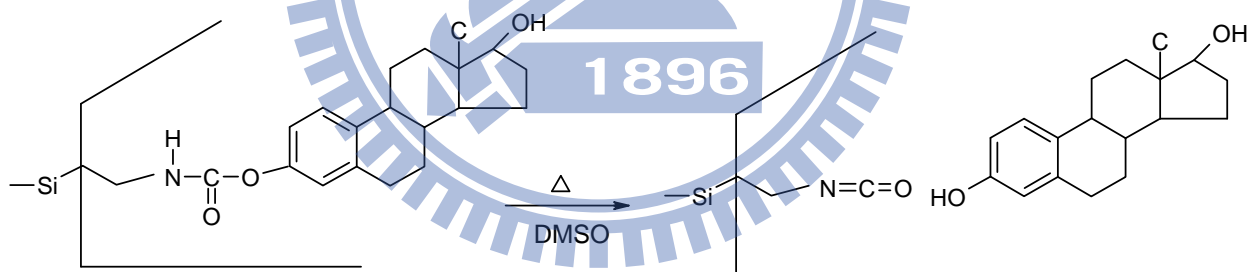
Figure 3- 4. Extraction of covalent bond and generation of a recognition site.

41

3-3 Characterization

3-3-1 Specific Surface Areas (BET)

The specific surface areas and pore volume of the hybrid materials were analyzed by N_2 adsorption technique and calculated using Brunauer-Emmett-Teller (BET) analysis. The 0.15 g of sample was degassed at 130 $^{\circ}$C for 8 hr before analysis. Nitrogen gas physisorption and desorption was measured at 77 k under variety of relative pressure (p/p$_o$) (Micromeritics, Tri Star 3000). This method is based on the determination of quantity of nitrogen necessary to completely cover the surface of sample. The trapped amount of N_2 gas was further applied to determine the total pore volume, which corresponded to the sum of the micropore and mesopore volume of samples. Relevant information of the average pore diameter could be obtained from the data of specific surface areas and total pore volume. In addition, each layer of adsorbate is treated as a Langmuir monolayer.

3-3-2 Fourier Transform Infrared Spectrometer (FTIR)

The Fourier transform infrared spectrometer (FTIR, Horiba, FT-730) was used to characterize the functional groups of polymers between 400 and 4000 wavenumbers (cm^{-1}). The samples were diluted with KBr and were pressed as self-standing pellets. The spectra were recorded with a resolution of 4 cm^{-1} for 100 times when pure KBr was employed as background.

3-3-3 Thermogravimetric Analysis (TGA)

The thermal property of MIPs was examined by a thermogravimetric analysis (TGA, TA instrument, Q500) to understand the changes of mass loss with the elevation of temperature. Measurements were taking from room temperature to 700 $^{\circ}$C at 10 $^{\circ}$C/min under air flow of 60 mL/min.

3-4 Adsorption

50 mg of particles were mixed with 5 mL E2/acetonitrile solution (150 mg/L) and shaker at room temperature for 4 hr. The solution was then centrifuged at 14000 rpm for 10 min. The adsorption capacity was determined by the reduced amount of E2 in the supernatant using a UV spectrometer (HITACHI U-3010). The absorption at 200-330 nm was recorded and the changes in absorption intensity at 280 nm were measured to calculate the concentration of E2. The amount of adsorbed E2 was calculated to obtain the adsorption capacity (K_d) of the MIPs by equation 3-1.

$$K_d(mg\ E2\ /\ g\ MIPs) = \frac{(C_o - C_e)V}{m}$$

(3-1)

Where C_o (mg/L) and C_e (mg/L) represented initial and equilibration concentration of E2, V (L) was the volume of solution, and m (g) was the weight of the imprinted polymers.

The imprinted factor (I) was calculated using equation 3-2.

$$I = \frac{K_{d(MIPs)}}{K_{d(NIP)}}$$

(3-2)

Where K_d (MIPs) and K_d (NIP) are the adsorption capacity of E2 on molecular imprinted and control polymer, respectively.

3-4-1 Equilibrium

Adsorption equilibrium of MIPs and related NIP toward E2 were determined by measuring the adsorbed amount of E2 in series sampling tubes at varies time intervals. 50

mg of samples were added to 5 mL of E2/acetonitrile solution (150 mg/L) in five tubes and mixed by shaker at room temperature.   Then, each of them was centrifuged at 14000 rpm for 10 min to remove the polymers.   The remaining concentrations of E2 in the supernatants were identified using UV-vis spectrometer.

3-4-2   pH effect

To understand the effect of pH values on the adsorption capacities, various pH (pH 3.2-7.2) were adjusted using HCl.   The E2 was dissolved into acetonitrile and then added into HCl solutions (acetonitrile/DI=50/50, v/v) with different pH values.   25 mg of the MIPs were added to 5 mL of the 150 mg/L E2 solutions in test tubes when different pH values were used.   The mixtures were shaken at room temperature for 4 hr and then centrifuged at 14000 rpm for 10 min.   The reduction of the concentrations of E2 in the supernatants was analyzed using UV-vis spectrometer, and the rebinding capacity was calculated using the equation 3-1.
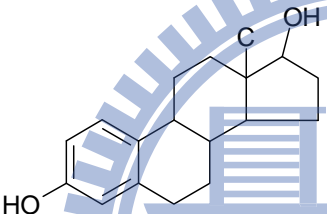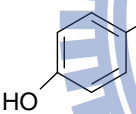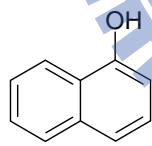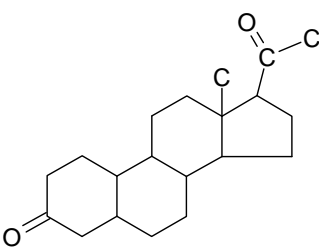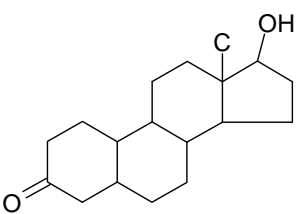
3-4-3   Solvents

To understand the effect of solvents on the adsorption capacities, various solvents including toluene, tetrahydrofuran, ethanol, acetonitrile, and methanol were used for the adsorption test.   The E2 was dissolved into the solvents and then used for the rebinding tests. 25 mg of samples were added to 5 mL of 150 mg/L E2 of vary solvents in a centrifuge tube when different solvents were used.   The mixtures were shaken at room temperature for 4 h and then centrifuged at 14000 rpm for 10 min.   The concentration of E2 in the supernatant was determined based the intensity of its characteristic absorption and the rebinding capacities were calculated using the equation 3-1.   The characteristic absorption changed a little bit in different solvents, and its appeared at 281.5 nm in ethanol, 280 nm for acetonitrile, 281 nm for methanol, 290.5 nm for tetrahydrofuran, and 288 nm for Toluene.

3-4-4 Selectivities

To understand the selective capability of MIPs for the target compound, analogues including nonylphenol, 1-naphthol, progesterone, and testosterone were selected to analyze the binding sites with E2.   The selective adsorption of MIPs was carried out in individual and mixed solution when acetonitrile was used as the solvent.   The physicochemical properties of E2 and its analogues were summarized in Table 3-2.

Table 3- 2. Physicochemical properties of compounds used for selective adsorptions test.

Compound	Chemical structure	Aqueous solubility	Log K_{ow}	Ref.
17β-estradiol (E2)		3.6 mg/L	4.01	76
Nonylphenol		4.9 mg/L	4.48	76
1-naphthol		870 mg/L	2.85	77
Progesterone		27 mg/L	3.67	78
Testosterone		23.4 mg/L	3.32	79

For individual compound adsorption, 25 mg of samples were added to 5 mL of 150 mg/L of E2, nonylphenol, and 1-naphthol, and 50 mg/L of E2, progesterone, and testosterone solutions individually and shaken at room temperature for 4 hr.   Then, the suspensions were centrifuged at 14000 rpm for 10 min.   The changed intensities of the characteristic absorptions of 1-naphthol, nonylphenol, progesterone, and testosterone at 323, 279, 237.5, and 238 nm respectively were taken to calculate their absorption capacities using the equation 3-1.   For completive systems, the 1-naphthol, nonylphenol, and E2 compounds were dissolved in acetonitrile to reach 150 mg/L for each one.   25 mg of MIPs was added to 5 mL mixture solution and shaken at room temperature for 4 hr, and then centrifuged at 15000 rpm for 10 min.   In order to remove the tiny suspending particles, the supernatant (3 mL) from the first centrifugation was transferred into another tube and underwent centrifugation at 15000 rpm for 20 min.   Following 1 mL of the supernatant was analyzed by HPLC (Agilent Technologies 1200 series) to determine the adsorption capacity of imprinted polymers toward the three compounds.   The compounds in mixtures were separated by a security guard column and an analytical reversed-phase column (Phenomenex LUNA, C18(2) column, 5 μm, 4.6×250 mm).   The eluent was 100% acetonitrile at a flow rate of 1 mL/min.   The injection volume was 50 μL, and the column effluent was monitored at 280 nm.   The selectivity factor (S) was determined by the equation 3-3:

$$ S = \frac{K_{d(E2)}}{K_{d(compound)}} \tag{3-3} $$

Where K_d (E2) and K_d (compound) are the adsorption capacity of MIP toward estradiol and tested compound.

Chapter 4. Results and Discussion

4-1 Optimization of constituents and sol-gel process of MIPs

4-1-1 Porogens

Porogens would cause significant influences on adsorption affinity of MIPs due to their polarity. To understand the effect of porogens on the adsorption capacity, three common organic solvents including ethanol, acetonitrile, and tetrahydrofuran were employed in the sol-gel process. The TEOS/PTMOS/E2 molar ratio was controlled at 20/2/1, when different porogens were used. Figure 4-1 shows the adsorption capacity of the MIPs toward E2 prepared under different porogens. The adsorption capacities of MIPs were 0.03 mg/g for ethanol, 0.12 mg/g for acetonitrile, and 0.07 mg/g for tetrahydrofuran. The highest adsorption capacity was appeared when acetonitrile was porogen. The polarity of three porogens were acetonitrile > ethanol > tetrahydrofuran.[80] Since the major interaction between E2 and PTMOS was dependent on hydrophobic interactions, polar porogen can promote the E2 bound to PTMOS to form well imprinted cavities. Ethanol would generate hydrogen bond to E2 and precluded interaction between PTMOS and E2, thereby resulting in the lowest adsorption capacity (0.03 mg/g). Therefore, acetonitrile was used as the major porogen for the following preparation of samples.
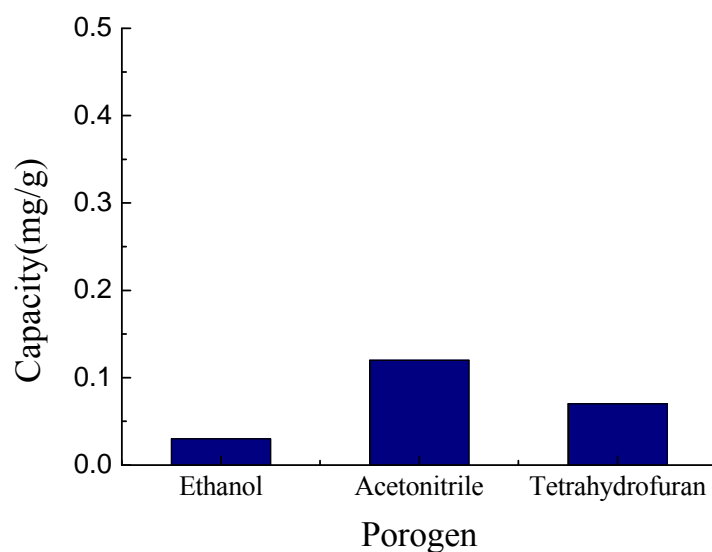
Figure 4- 1. The adsorption capacities of the MIPs prepared by ethanol, acetonitrile, and tetrahydrofuran.

4-1-2 Functional monomers

One of the basic demands for successful imprinted process is the presence of functional monomers appropriate in the polymer matrix. The role of those monomers is to create recognition sites by leaving interacting chemical functional groups in cavity for rebinding. To increase adsorption affinity, varieties functional monomers were used in polymerization process. The PTMOS was chosen to interact with E2 by π-π stacking and hydrophobic interactions, and APTES bonded with E2 through hydrogen bonds. In addition, the MTMOS was used to enhance the hydrophobicity and elasticity of the MIPs. Table 4-1 shows the different combinations of functional monomers used for preparation of MIPs. Figure 4-2 shows the binding affinity of E2 by both of MIPs and their related NIP. The adsorption capacity of T, TA, TP, TAP, TPM, and TAPM was 0.03, 0.17, 0.12, 0.23, 0.09, and 0.36 mg/g, and imprinted factors were 1.5, 0.9, 12, 1.8, 4.5, and 1.8, respectively. The samples comprising APTES such as TA, TAP, and, TAPM, exhibited better adsorption

48

capacity than the samples without APTES such as TP and TPM. This was because the high specific surface areas induced by APTES (more than 400 m^2/g of three samples). However, the lowest imprinted factor was observed in TA which was only composed TEOS and APTES. This was because that the hydrogen bonding of E2 with the amino group of APTES was competed by Si-OH groups and inadequate for E2 imbedded into network. Consequently, the structure of specific cavities for E2 poorly constructed and their quantities decreased in the MIPs.

When PTMOS was used as the functional monomer, the adsorption capacity of TP for E2 was comparatively low due to lower specific surface areas (96 m^2/g). However, the TP performed the highest imprinted factor. This reveals that strong π-π stacking interaction facilitates the formation of imprinted sites for E2. This contribution was confirmed in TAP when PTMOS and APTES were both used as the functional monomers. The TAP showed a higher imprinted factor than TA. Marx et al. have reported that the hydrogen bonds established between APTES and parathion were week to produce imprinted cavities whereas the combination of PTMOS and APTES with TEOS caused a synergistic effect for imprinted cavities.[71] Moreover, the presence of APTES improved the adsorption capacity of TP. Therefore, the imprinted factor and texture of the MIPs were attributed by PTMOS and APTES, respectively.

On the other hand, MTMOS was used to enhance hydrophobicity and flexibility of TAP.[44, 48] TAPM indeed showed the improved adsorption capacity than TAP. However, it did not promote the imprinted factor of TAP. This finding indicates that the MTMOS mainly increased the non-specific binding through hydrophobic interaction. Actually, the binding capacity of TP was reduced by addition of MTMOS. The phenomenon suggested that competitive hydrophobic interaction of methyl groups interfered with the π-π stacking between phenyl and E2. However, the presence of APTES reduced the effects in the TAPM sample. Thus, the imprinted cavities mainly contained amino- and phenyl groups, while the

methyl groups existed in the non-specific binding sites.

Table 4- 1. The MIPs prepared by different compositions of functional monomers.

| Samples | Molar ratios | | | | |
	TEOS	APTES	PTMOS	MTMOS	E2
T	20	--[a]	--	--	1
TA	20	2	--	--	1
TP	20	--	2	--	1
TAP	20	2	2	--	1
TAPM	20	2	2	2	1
TPM	20	--	2	2	1

[a] indicates no monomers involved in preparation process.

Figure 4- 2. The adsorption capacities of the MIPs (dark bars) and their corresponding NIP (light bars) prepared by combination of functional monomers. The error bar was obtained by 4 tests.

4-1-3　Cross-linkers

To understand the effect of cross-linkers on adsorption ability, the molar ratios of TEOS was changed in sol-gel process.　The TEOS/E2 molar ratios were increased from 20 to 60, and the APTES/PTMOS/E2 molar ratio was controlled at 2/2/1.　Figure 4-3 shows the adsorption capacity of MIPs and their related NIP prepared by different TEOS/E2 ratios. The adsorption capacities decreased from 0.36 to 0.17 mg/g when the TEOS/E2 ratios increased from 20 to 60.　Meanwhile, the imprinted factors kept at 1.4-1.8, irrespective to the changes of the TEOS/E2 ratios.　More TEOS used in the fabrication of materials decreased the density of recognition sites so as the adsorption capacity.　Moreover, higher contents of hard silica caused the difficult diffusion of E2, thereby limiting its future applications.　The NIP also possessed the same tendency as the MIPs because of reduction of the non-specific binding sites due to the increased silica.

Figure 4- 3. The adsorption capacities of the MIPs (dark bars) and their corresponding NIP (light bars) prepared by different TEOS/E2 ratios.　The APTES/PTMOS/E2 was controlled at 2/2/1.　The error bar was obtained by 4 tests.

4-1-4　TEOS/MTMOS ratios

E2 contains high hydrophobicity and is more soluble in organic solvent than in water because of its high log K_{ow} = 4.01.[81]　This character makes E2 probably not accommodated in hydrophilic sol-gel-derived matrix.　Assessment of molecularly imprinted sol-gel materials for selective recognition of nafcillin was published by L. Guardi et al.　It showed that the presence of favorable hydrophobic interaction between nafcillin and the sol-gel host improved the affinity of analyte.　For creating more recognition sites, the MTMOS was used to increase the hydrophobicity of imprinted polymers by methyl group.[48, 49]　The TEOS/MTMOS molar ratios were decreased from 10 to 0.1, while APTES/PTMOS/E2 molar ratio was controlled at 2/2/1.　Figure 4-4 shows the adsorption capacity of MIPs and their corresponding NIP under different TEOS/MTMOS ratios.　The adsorption capacities were ranged 0.28-0.36 mg/g whereas the imprinted factors decreased from 1.8 to 0.9 as the TEOS/MTMOS ratio decreased from 10 to 0.1.　Interestingly, the changes in the adsorption ability were negligible while the samples were more hydrophobic due to the methyl group of MTMOS.　This indicated that more MTMOS replaced TEOS in material was inefficiently to form the rigid cavities for E2 due to the lack of hard structure.[20]　Therefore, it increased the non-specific adsorption ability and reduced imprinted factor.　It was differed from L. Guardi et al. study.　This finding clearly demonstrated that the generation of imprinted cavities was mainly determined by phenyl and amino groups.
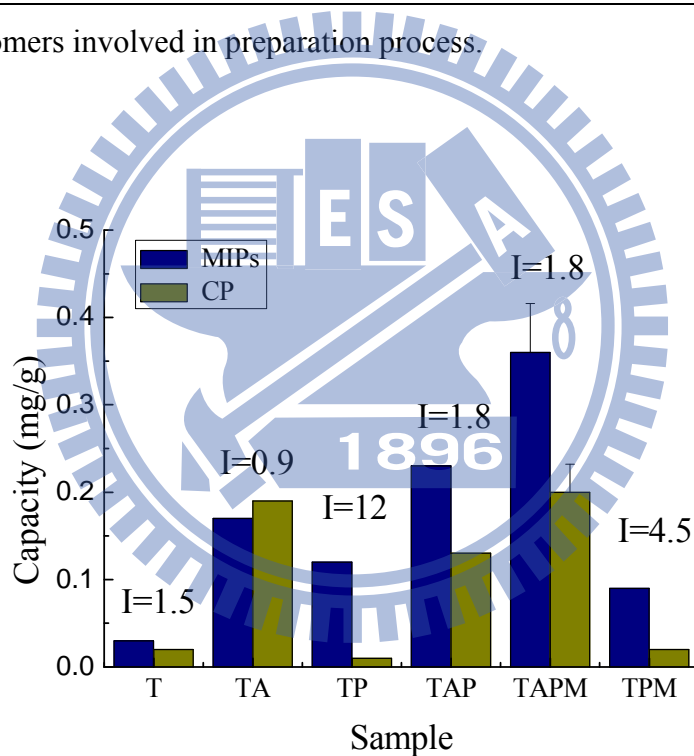
Figure 4- 4. The adsorption capacities of the MIPs (dark bars) and their corresponding NIP (light bars) prepared by different TEOS/MTMOS ratios. The APTES/PTMOS/E2 was controlled at 2/2/1. The error bar was obtained by 4 tests.

4-1-5 Catalysts

In the sol-gel process, the prompt gelation was observed when APTES was added to the hydrolyzed TEOS solutions. This might cause heterogeneous of matrix. To retard the gelation, acetic acid was used to replace HCl as the catalysts in the sol-gel process because of its low acidity. Figure 4-5 shows the capacity results of TA, TAP, and TAPM and their corresponding NIP catalyzed by acetic acid. The new samples were named as TAc, TAPc, and TAPMc to make the difference from the samples catalyzed by HCl. The results indicated that the adsorption capacities of TAc, TAPc, and TAPMc were 0.04, 0.01, and 0.02 mg/g, and the imprinted factors were 1.3, 0.3, and 2.0, respectively. These adsorption capacities of TAc, TAPc, and TAPMc with HAc catalytic were much lower than those of TA (0.17 mg/g), TAP (0.23 mg/g), and TAPM (0.36 mg/g) catalyzed by HCl. This was because the lower specific surface areas were resulted in HAc catalyzed sol-gel process. The specific surface areas of TAc, TAPc, and TAPMc were 30, 41, and 35 m^2/g, which were all

53

lower than 543 m^2/g of TA, 419 m^2/g of TAP, and 513 m^2/g of TAPM. The low acidic

strength of HAc and chelating of the −COO$^-$ to Si centers slow gelation rate, thereby resulting

in lower specific surface areas.   In addition, HAc might disrupt interaction between APTES

and E2 by forming stronger hydrogen bonding with amino group than E2 to reduce the
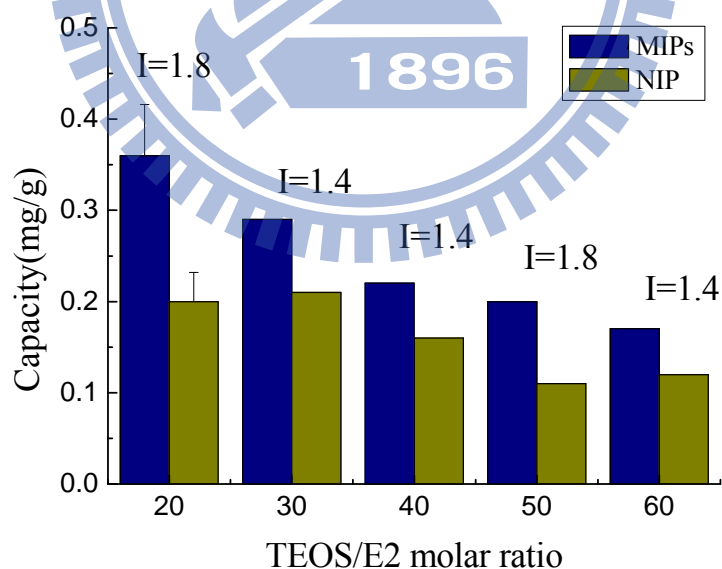
imprinting effect, thereby reducing the specific adsorptions.

Figure 4- 5. The adsorption capacities of the MIPs (dark bars) and their corresponding NIP

(light bars) prepared by HAc catalyzed sol-gel process.

4-1-6   Water/Si ratios

Water contents determine the gelation rate and the final structure of sol-gel-derived

materials, thus they could influence the adsorption of MIPs.   In this study, the adsorption

behaviors of the MIPs prepared by different water/Si were examined.   The water/Si ratios

were adjusted from 5 to 0.5 when the TEOS/APTES/PTMOS/MTMOS/E2 molar ratio was

controlled   at   20/2/2/2/1.   Actually,   the   water/Si   molar   ratio   was   calculated   by

water/TEOS+3/4(APTES+PTMOS+MTMOS).　Figure 4-6 shows the adsorption capacity of MIPs and their corresponding NIP under different water/Si ratios.　The adsorption capacities increased from 0.36 to 0.44 mg/g when the water/Si ratios decreased from 5.0 to 3.3. Meanwhile, the imprinted factors kept at 1.8-1.9.　The adsorption capacities decreased from 0.44 to 0.10 mg/g whereas the imprinted factors increased from1.9 to 10.0 as the water/Si ratios decreased from 3.3 to 0.5.　The highest adsorption capacity was occurred at the water/Si of 3.3.　The decreased in adsorption capacity when the water/Si decreased from 5.0 to 3.3 was attributed to the high affinity of APTES with water.　When the water content decreased, it was favor for the interaction between APTES and E2.　It is noted that the adsorption capacity decreased when the water/Si ratio was below 3.3, indicating that incomplete hydrolysis of sol-gel process decreased the quantities of imprinted cavities. However, the high imprinted factor occurred at water/Si=0.5 indicated that the non-hydrolyzed organic branch assisted the formation of imprinted cavities because of increased hydrophobicity in the sol-gel process.　Under this condition, hydrophobic E2 could entirely embed to precursor sol, and produce the integrated imprinted cavities.[34]
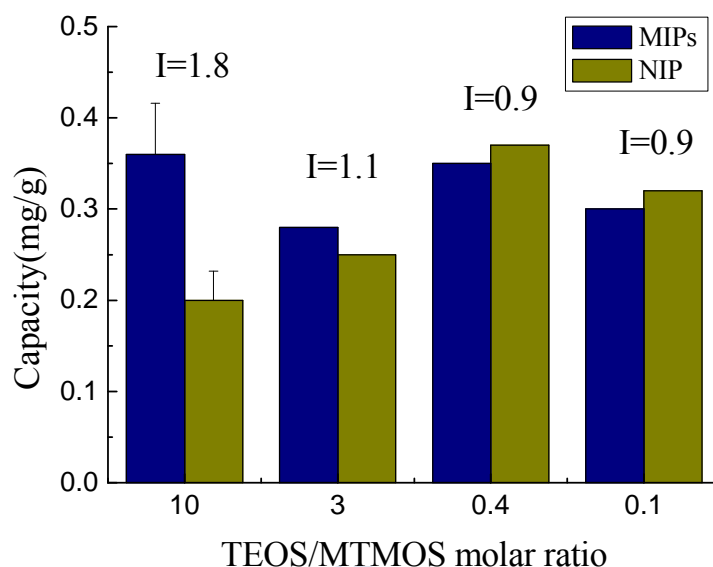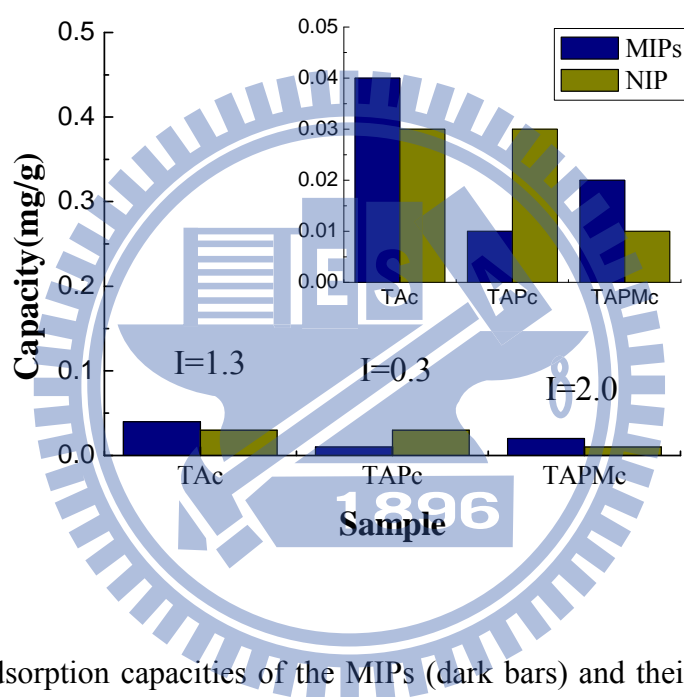
Figure 4- 6. The adsorption capacities of the MIPs (dark bars) and their corresponding NIP (light bars) prepared by different water/Si ratios.   The TEOS/APTES/PTMOS/MTMOS/E2 was controlled at 20/2/2/2/1.

4-1-7   pH values

Since the structures of sol-gel-derived MIPs are pH dependent, the influence of pH on the adsorption cavities and imprinted factors of the samples was elucidated.   The pH values of sol solutions were varied from 1 to 4 when the water/Si molar ratio was controlled at 3.3 and the TEOS/APTES/PTMOS/MTMOS/E2 molar ratio controlled at 20/2/2/2/1.   Figure 4-7 shows the adsorption capacities of MIPs and their corresponding NIP prepared under different pH values.   The adsorption capacities decreased from 0.44 to 0.13 mg/g whereas the imprinted factors were ranged 1.7-2.6 as the pH decreased from 4 to 1.   There were similar adsorption capacities and imprinted factors when the pH values ranged 3-4 during the sol-gel process presumably due to the similar gelation rate.   However, the adsorption capacity was decreased when the pH value was lower than 3.   This finding reveals that the protonation of amino groups of APTES weaken the interaction between the amino groups and E2.[82]   F Li et al. prepared a molecularly imprinted polymer grafted on polysaccharide

microsphere surface by the sol-gel process for protein recognition.   They found low protein re-adsorption capacities at pH=2 due to the inefficient imprinting.[20]   Thus, the quantities of imprinted cavities were decreased due to the template was inefficiently embedded into silica matrix.[20]   It is noted that the highest adsorption capacity of the organic-inorganic MIPs for E2 (0.44 mg/g) in this study was higher than that of the organic MIPs (0.18 mg/g) prepared by H. Dong et al.[83]   Thus, the organic-inorganic MIPs are more promising than the traditional organic ones for real applications.
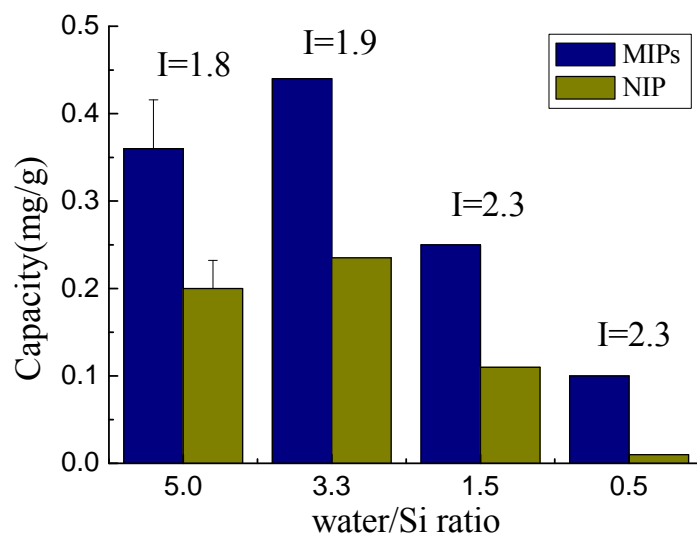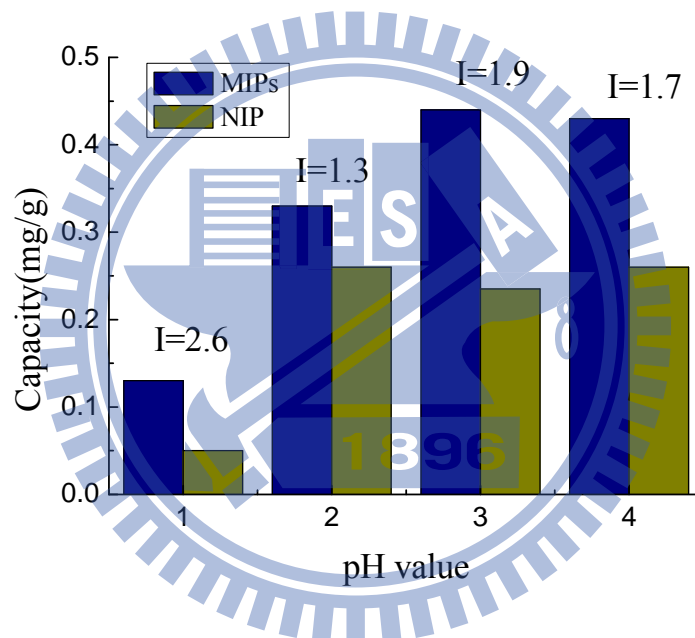

Figure 4- 7. The adsorption capacities of the MIPs (dark bars) and their corresponding NIP (light bars) prepared by different pH values.   The water/Si ratio was controlled at 3.3 and the TEOS/APTES/PTMOS/MTMOS/E2 was controlled at 20/2/2/2/1.

4-2   Characterizations

4-2-1   Functional groups

Figure 4-8 shows the FTIR spectra of the MIPs prepared by different functional monomers.   The O-H stretching of physisorbed water were observed in the 3400-3200 cm^{-1} region.[15]   The strong bands at 1167 cm^{-1} and 1075 cm^{-1} could be attributed to the Si-O-Si asymmetric stretching.[16]   Other bands correspond to Si-O of SiO_2 were presented at 781 cm^{-1} and 470 cm^{-1}, and to −OH vibrations in bulk gel was at 1636 cm^{-1}.[15, 39]   A characteristic feature of TA compared with TP and TPM was N-H band near 1560 cm^{-1}.   The benzene ring absorptions at 735 cm^{-1} and 691 cm^{-1} were observed in TP and TPM.[51]   Moreover, TPM contained Si-CH_3 bands at 1288 cm^{-1}.[84]   These FTIR spectra confirmed that all the functional monomers used in the preparation were successfully incorporated in the framework of MIPs.
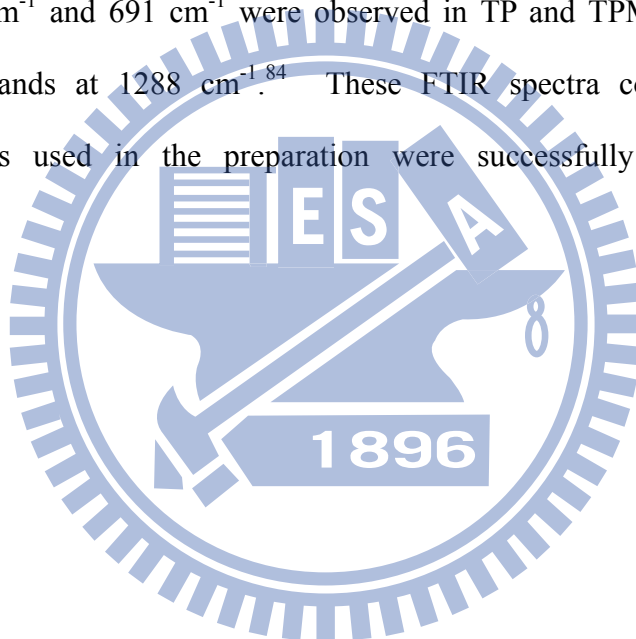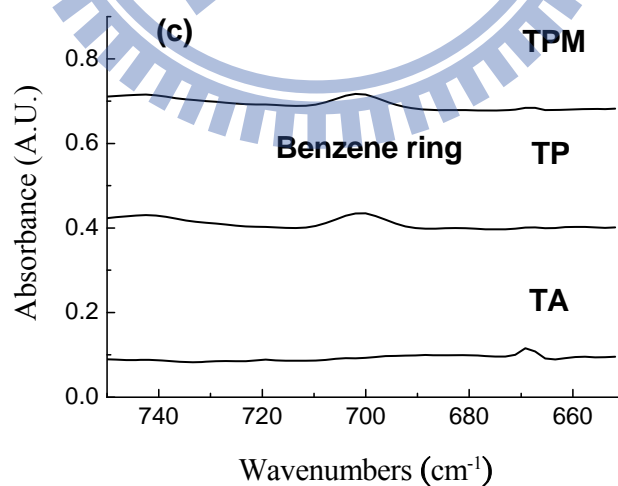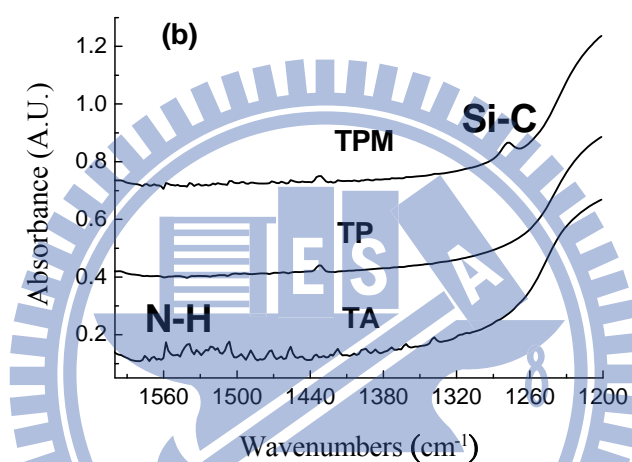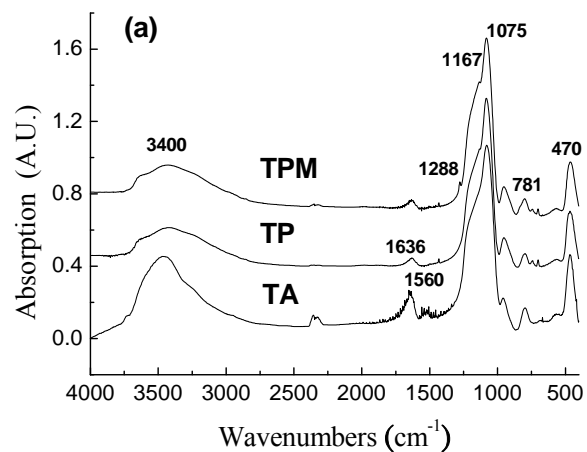
Figure 4- 8. IR spectra of TA, TP, and TPM with wavenumbers between 4000-400 cm^{-1} (a), and (b) and (c) are the augmentation of the IR spectra in 1200-1600 cm^{-1} and 750-650 cm^{-1}, respectively.

Figure 4-9 shows the FTIR spectra of E2, the TAPM under as-prepared, after extraction, and after re-binding conditions, and its corresponding NIP. The significant peak at around 2980 to 2830 cm^{-1} contributed by E2 appeared in TAPM as-prepared but disappears after extraction and adsorption of E2. It low rebinding capacity of MIPs led little absorptions of the characteristic bands after adsorption of E2. On the other hand, the water absorption was increased after extraction process due to the formation of imprinted cavities. Compare to NIP, TAPM exhibited high intensity for water absorption in the 3400-3200 cm^{-1} region. The high quantities of adsorbed water again evidenced the artificial cavities existing in the imprinted polymers.
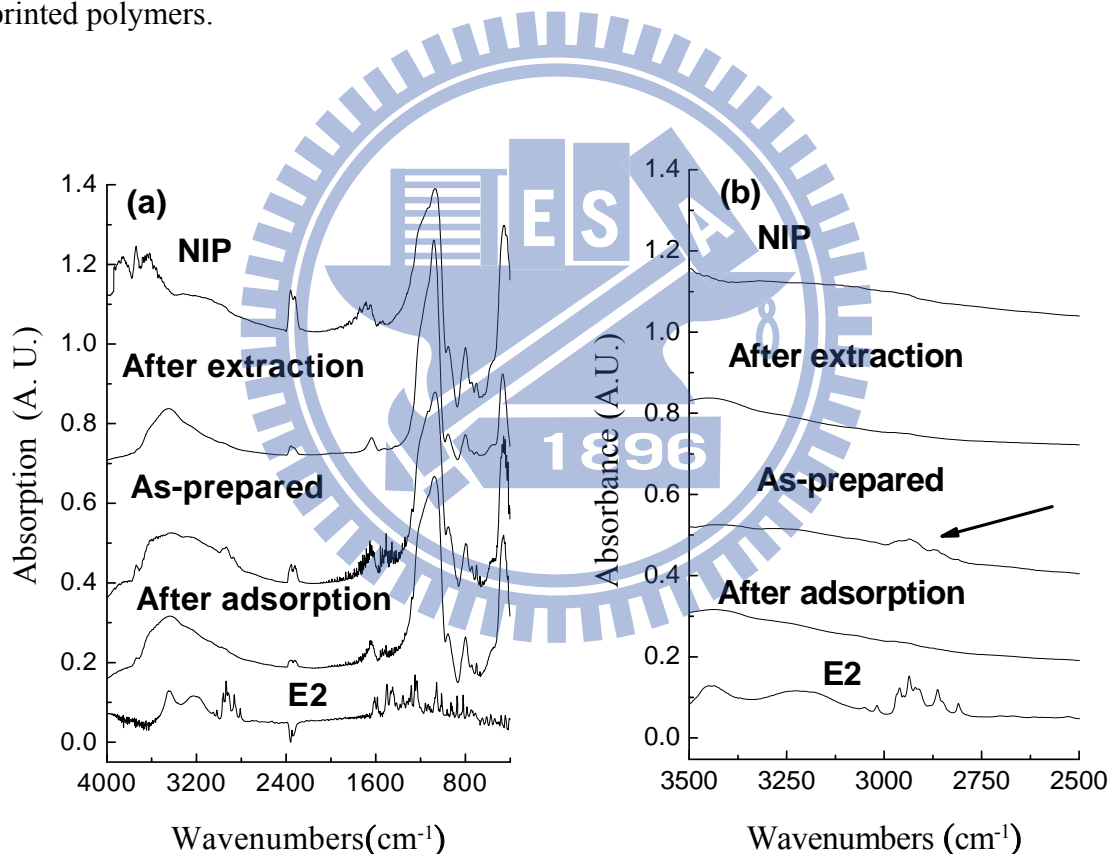
Figure 4- 9. The FTIR spectra of (a) E2, the TAPM under as-prepared, after extraction, and after re-binding conditions, and its corresponding NIP at 4000-400 cm^{-1} and (b) the magnification of the IR spectra at 2500-3500 cm^{-1}.

4-2-2 Textures

The specific surface areas played an important role in adsorptions. High specific surface areas could provide more active site to bind analytes in adsorption processes. Table 4-2 summarizes the BET specific surface areas of samples prepared by different combinations of functional monomers. The specific surface areas of samples were 96 m^2/g for TP, 543 m^2/g for TA, 229 m^2/g for TPM, 419 m^2/g for TAP, and 513 m^2/g for TAPM. Higher specific surface areas (> 400 m^2/g) were obtained when APTES were involved in the samples. The increased specific areas were caused by rapid gelation. The basic properties of the amino group in the APTES formed the internal hydrogen bonds with the silanol groups and consequently promoted hydrolysis and condensation rates.[85,86] On the other hand, MTMOS also greatly increased the specific surface areas of TP and TAP from 96 m^2/g and 419 m^2/g to 229 m^2/g (TPM) and 543 m^2/g (TAPM), respectively. Substitution of an ethoxy group with methyl group was increased hydrolysis rate by polar effect. The TP sample exhibited the lowest specific surface areas. Moreover, addition of PTMOS decreased the specific surface areas of TA from 543 m^2/g to 419 m^2/g (TAP). These results were due to the steric effect of phenyl group slow gelation down gelation rates.

Table 4- 2. The BET specific surface areas of samples prepared by different combinations of functional monomers.

Samples	Specific surface areas (m^2/g)
TP	96
TA	543
TPM	229
TAP	419
TAPM	513

The highest adsorption capacity and good imprinted factor was exhibited in sample W3.3 which was prepared at TEOS/APTES/PTMOS/MTMOS/E2=20/2/2/2/1, water/Si=3.3 and pH=3. Figure 4-10 shows the nitrogen adsorption-desorption isotherm of W3.3 and its corresponding NIP. The W3.3 had a combination of type I/IV isotherm, corresponding to mesoporous materials with a well-developed microporosity.[47] The isotherm shape of NIP was displayed as type I isotherm, indicating micro and macroporous features of the material. The result indicated that the presence of the template during the preparation process occupied some space. After removal of the template from the MIPs, the imprinted cavities were successful left in the silica network. The hysteresis loop of W3.3 was shown as the typical H_2 type in IUPAC classification, indicating the pores containing constriction, commonly found in silica.[47, 87] The formation of irregular pores should be caused by the aminopropyl groups incorporated the pores.
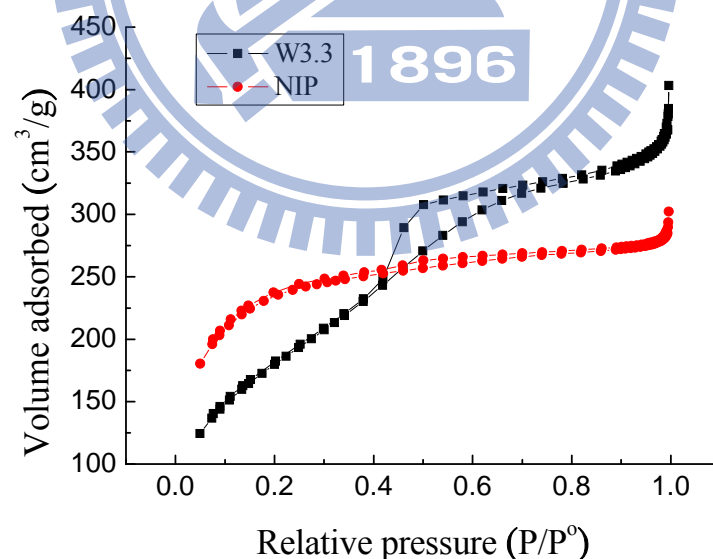
Figure 4- 10. N_2 adsorption-desorption isotherms of W3.3 (solid square) and its corresponding NIP (solid cycle).

Table 4-3 lists the specific surface areas and pore volume data of W3.3 and its corresponding NIP under as-prepared, after extraction, and after adsorption conditions. The specific surface areas of as-prepared W3.3 were 288 m^2/g, which were much smaller than that of as-prepared NIP (813 m^2/g). The presence of templates caused the steric effect in sol-gel process and slowed down gelation rate. The specific surface areas of NIP was only slightly increased from 814 m^2/g to 832 m^2/g after extraction process due to some unreacted chemicals, such as sol-gel precursor or monomers, were washed out from the material.[88] However, the specific surface areas and pore volume of W3.3 increased significantly from 288 m^2/g to 658 m^2/g and 0.25 m^2/g to 0.59 cm^3/g, respectively, after extraction. The results clearly revealed that removing template created additional pores in the silica matrixes, resulting in increased in both specific surface areas and pore volume. In addition, the reduction of the weight of materials was increased the specific surface areas of MIPs by removal of template. After rebinding of E2, the specific surface areas and pore volume of W3.3 were decreased from 658 m^2/g and 0.59 cm^3/g to 539 m^2/g and 0.55 cm^3/g, respectively. Similar phenomenon was observed in the NIP sample, in which the specific surface areas and pore volume decreased from 832 m^2/g and 0.48 cm^3/g to 497 m^2/g and 0.45 cm^3/g, respectively, after adsorption of E2. These reductions evidenced the rebinding of E2 occurred the pores of MIPs and NIP samples.

Table 4- 3. Profiles of samples for extraction effects test.

Samples		Specific surface areas (m^2/g)	Pore volume (cm^3/g)
W3.3	as-prepared	288	0.25
	after extraction	658	0.59
	after adsorption	539	0.55
NIP	as-prepared	813	0.62
	after extraction	832	0.48
	after adsorption	497	0.45

4-2-3　Recovery

Figure 4-11 shows the thermal behaviors of W3.3 and its corresponding NIP at elevated temperature from room 25 to 700 ^{o}C.　The weight loss of TGA curve was divided into three regions: room temperature-150 ^{o}C, 150-400 ^{o}C, and 400-700 ^{o}C.　Between room temperature and 150 ^{o}C, the weight loss was attributed to the removal of surface physisorbed water or organic solvent from materials.[89]　The weight loss at 150-400 ^{o}C was due to the thermal decomposition of the APTES, MTMOS and template or the condensation between silanol groups.　Furthermore, the weights loss between 400-700 ^{o}C was mainly due to the thermal decomposition of PTMOS and removal of surface hydroxyl groups via dehydroxylation.[90, 91]
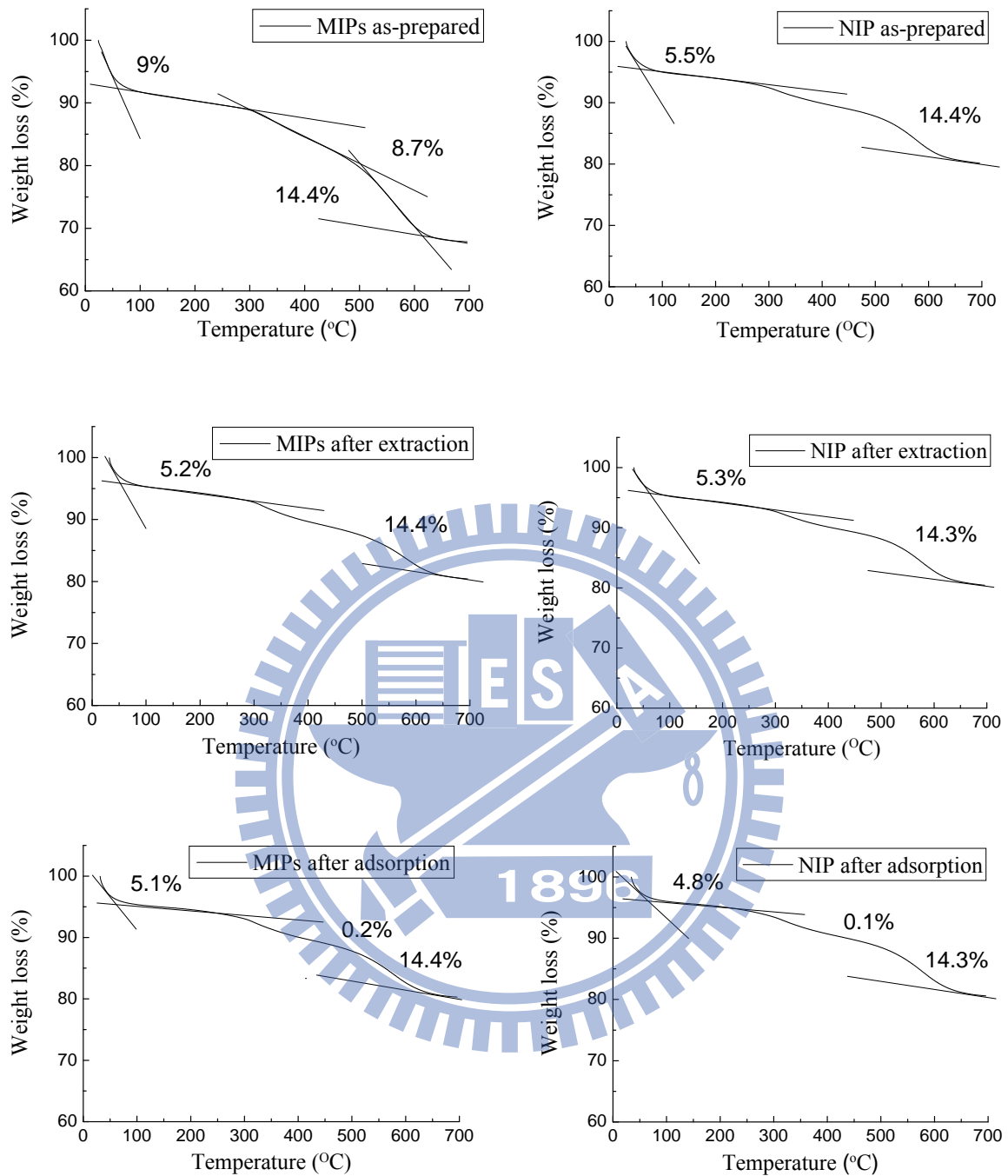
Figure 4- 11. The weight loss of W3.3 and its related NIP toward E2 for extraction test.

Table 4- 4. The composition of MIPs and its corresponding NIP for extraction test.

	Water (%)	E2 (%)	Monomers (%)	SiO$_2$ (%)
As-prepared				
MIPs	9	8.7	14.4	67.9
NIP	5.5	--[a]	14.4	80.1
After extraction				
MIPs	5.2	--	14.4	80.4
NIP	5.3	--	14.3	80.4
After adsorption				
MIPs	5.1	0.2	14.4	80.3
NIP	4.8	0.1	14.3	80.8

[a] indicates not available by TGA.

Table 4-4 lists the composition of MIPs and its corresponding NIP for extraction test. The composition of MIPs as-prepared was including water, E2, monomers, and SiO$_2$ and the composition of NIP as-prepared was the same with MIPs as-prepared without E2. The water and SiO$_2$ content were 9% and 67.9% for MIPs as-prepared and 5.5% and 80.1% for NIP as-prepared, respectively. It was assumed the monomers were the same among two samples. Therefore, the E2 content of MIPs as-prepared was 8.7%. The water content and SiO$_2$ content of MIPs after extraction were 5.2% and 80.4%. After calculation, the monomers content of MIPs as-prepared was consistent with the monomers of MIPs after extraction (14.4%). However, the monomers content of NIP as-prepared (14.3%) was slightly low than NIP after extraction (14.4%) due to some unreacted chemicals. This result was corresponding with BET analysis. The water and SiO$_2$ content of MIPs after adsorption were 5.1% and 80.3%. So, the E2 content of MIPs after adsorption was 0.2% when the monomers were equivalent. The recovery of MIPs was 2.3% in this study. The results

revealed that low recovery was caused by aggregation of E2 in preparation process. The similar phenomenon was observed in cholesterol imprinted inorganic materials prepared by Fujiwara et al.[92] Thus, there were few imprinted cavities created during sol-gel process, presumably due to high hydrophilicity of the SiO_2 matrix. Compared to microporous NIP, mesoporous MIPs obtained by N_2 adsorptions confirmed that E2 oil droplets existed in silica matrix. In addition, the pore volume of MIPs was slightly decreased from 0.59 to 0.55 cm^3/g after adsorption due to only few micropores were occupied.

4-3　Adsorption

4-3-1　Equilibrium

Figure 4-12 shows the accumulated adsorption capacities of W3.3 and its corresponding NIP for E2 in the different time intervals. The rebinding of NIP toward E2 quickly reached to saturation after 1 hr because the non-specific interaction mainly occurred at the surface. However, the long saturation period of 4 hr was observed in MIP due to the diffusion of E2 from surface into the cavities. Comparing with organic MIPs with a saturation time of more than 12 hr,[83] the organic-inorganic hybrid MIPs was showed efficient uptake for target compounds. This phenomenon was attributed to the high porosity of inorganic network of MIPs, which was facilitated adsorption of E2 into polymers.[52]
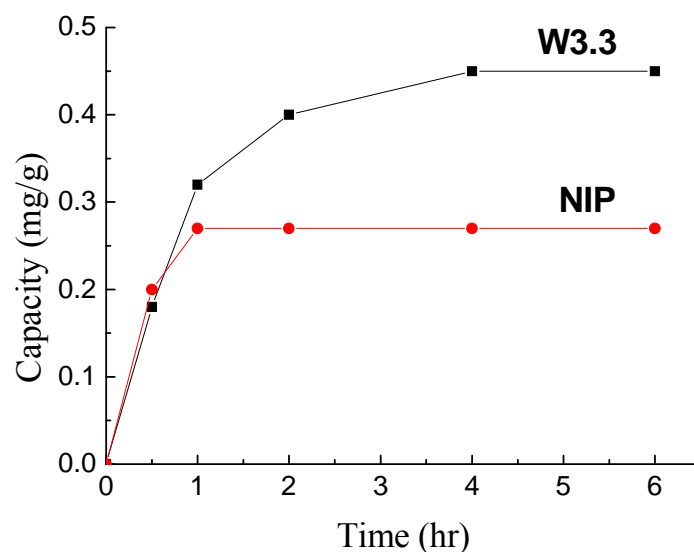
Figure 4- 12. The adsorption capacities of W3.3 and its corresponding NIP toward E2 in the regular time intervals ranged from 30 min to 6 hr.

4-3-2 pH

To understand the effect of pH values on the rebinding capacities, the pH values of E2 solutions were adjusted from 3.2 to 7.2. Figure 4-13 shows the adsorption capacities of the MIPs and its corresponding NIP in different pH values. The adsorption capacities were ranged 0.32-0.44 mg/g and the imprinted factors ranged 1.8-3.2. The similar rebinding capacities indicated that the electrostatic attraction between E2 and MIPs was insignificant in rebinding. In addition, the imprinted cavities maintained its structural stability against the pH values.
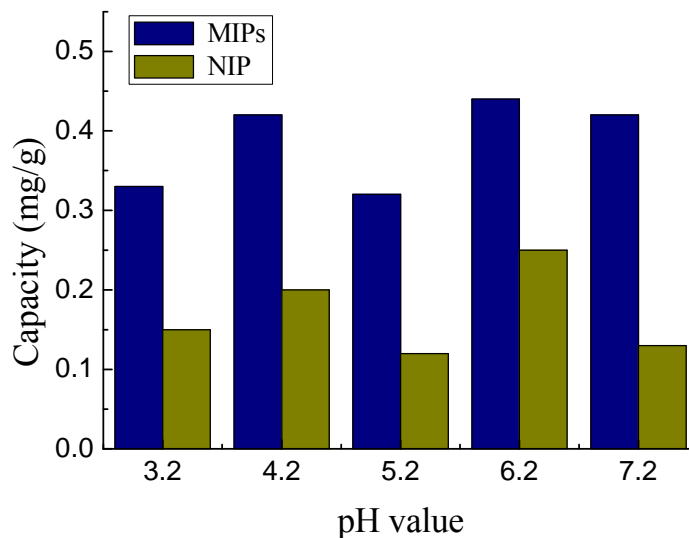
Figure 4- 13. The adsorption capacities of the W3.3 (dark bars) and its corresponding NIP (light bars) rebinding of E2 in varies pH solution ranging from 3.2 to 7.2.

4-3-1 Solvents

The interaction of E2 with imprinted polymers was investigated in various polar and apolar solvent. Figure 4-14 exhibits the binding of E2 to W3.3 in toluene, tetrahydrofuran, ethanol, methanol, and acetonitrile. The highest adsorption capacities of W3.3 were 28.2 mg/g in toluene, whereas the adsorption capacities in other solvents were in the ranged 0.06-0.44 mg/g. The imprinted factors of W3.3 in all solvents ranged between 1.8 and 2.6. The similar imprinting factors reveal that the changes in the adsorption capacities of MIPs were mainly contributed by different properties of the solvents. Marx and Liron reported that the rebinding of propanolol in polar solvent were high due to the stronger hydrophobic interaction in polar solvent.[50] The polarity of the solvents in this study followed the order toluene < tetrahydrofuran < acetonitrile < ethanol < methanol.[80] However, the binding of E2 was noticeably decreased with increasing solvent polarity. This phenomenon reveals that the functional groups of solvents dominated the adsorption of E2 in the MIPs. Since these polar solvents all can form hydrogen bonding with amino groups, the occupation of the

functional groups by the polar solvents decreased their binding toward E2. In contrast, the toluene assists the diffusion of E2 to the imprinted cavities because of π-π stacking interactions.
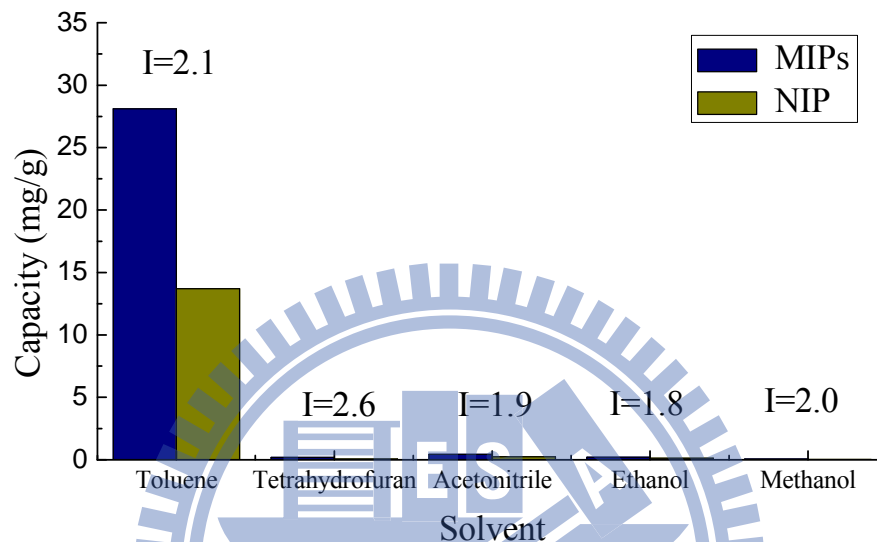
Figure 4- 14. The adsorption capacities of the W3.3 (dark bars) and its corresponding NIP (light bars) rebinding in varies polar and apolar solvent.

4-3-4 Selectivities

In order to evaluate the specific cavities affinity of MIPs toward to target compounds, selective adsorptions in single and mixing analogues solution were carried out. Nonylphenol, progesterone, testosterone, and 1-naphthol were chosen as the analogues for the selective adsorption test because the similar log K_{ow} and chemical structure to the target compound, E2.
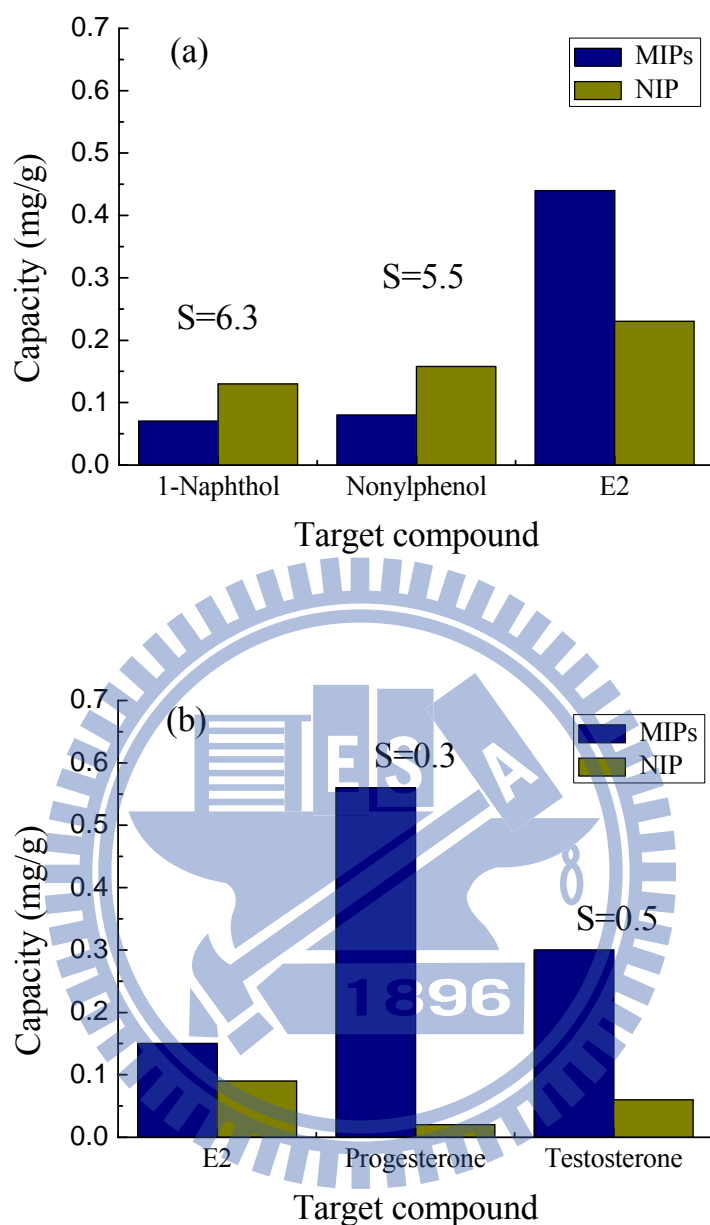
Figure 4- 15. The adsorption capacities of the MIPs (dark bars) and its corresponding NIP (light bars) for (a) 150 mg/L of 1-naphthol, nonylphenol, and E2 and (b) 50 mg/L of E2, progesterone, and testosterone in single adsorption.

Figure 4-15 shows the individual adsorption results of W3.3 and its corresponding NIP for E2, 1-naphthol, nonylphenol, progesterone, and testosterone. The adsorption capacity of the MIPs was 0.07 mg/g for 1-naphthol, 0.08 mg/g for nonylphenol, 0.56 mg/g for

progesterone, and 0.30 mg/g for testosterone.   The adsorption capacity of the MIPs toward 150 mg/L and 50 mg/L of E2 were 0.44 and 0.15 mg/g, respectively.   The MIPs showed the high selectivity factors of 6.3 for 1-naphthol and 5.5 for nonylphenol, whereas it is hard to distinguish steroid compound progesterone (S= 0.3) and testosterone (S= 0.5).   The results demonstrated that the imprinted cavities could recognize the target compound from structural similarity.   However, the lack of strong interactions between functional groups resulted in poor recognition ability to discriminate E2 from the analogues only with different substituent. The adsorption capacity of MIPs toward the steroid compounds were progesterone > testosterone > E2.   This phenomenon was resulted from the hydroxyl substituent.   E2 which contain 2 OH groups exhibited higher solubility in ACN because of stronger hydrogen bonding, while testosterone and progesterone which have only one and no OH group, respectively, showed lower affinity with the solvent and were easily trapped by the imprinted cavities.   Therefore, it evidenced again that the interaction between solvent and analyses interfered the adsorption ability of MIPs.   In addition, progesterone and testosterone do not have phenyl groups.   The low non-specific interaction for these two compounds but relatively higher adsorption of E2 in the NIPs reveal that the π-π stacking interaction really participated in the formation of imprinted cavities.   However, the geometry of the imprinted cavities contributed more to the recognition than the functional groups.
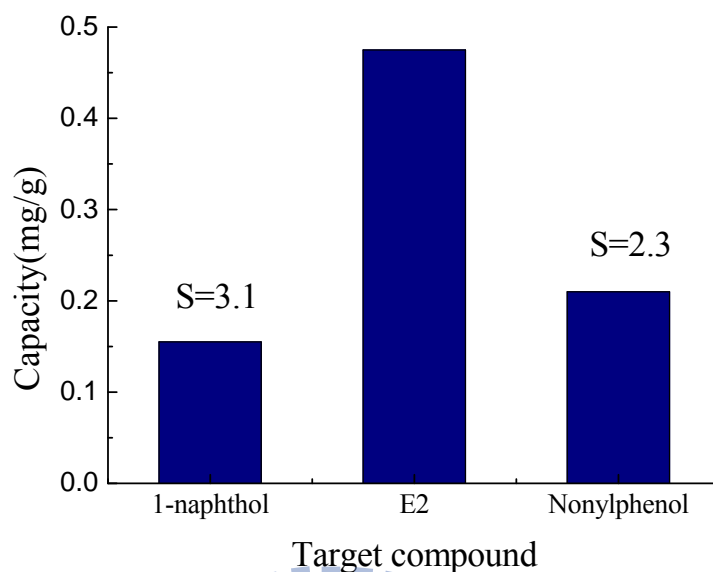
Figure 4- 16. The adsorption capacities of the MIPs for E2, nonylphenol, and 1-naphthol in mixed adsorption.

Figure 4-16 shows the adsorption capacities of W3.3 for E2, nonylphenol, and 1-naphthol in mixed adsorption. The concentrations of these three compounds were all controlled at 150 mg/L in acetonitrile. The adsorption capacity of MIPs in the competitive system was 0.155 mg/g for 1-naphthol, 0.475 mg/g for E2, and 0.21 mg/g for nonylphenol. The corresponding selectivity factor was 3.1 for 1-naphthol and 2.3 for nonylphenol. This result evidenced that the MIPs exhibited preferential adsorption toward the target compound. Compared to individual adsorption, the selectivity factor of 1-naphthol and nonylphenol were slight decreased in mixed solution. This was resulted from cross-interaction among the adsorbed compounds. The high selectivity factors reveal that the MIPs can strongly distinguish the target compound from analogues through recognizing sizes and shapes.

Chapter 5.   Conclusions

In this study, molecularly imprinted E2 organic-inorganic hybrid was successfully fabricated by a sol-gel process when APTES and PTMOS were as functional monomers.   In addition, high recognition capacity of MIPs for E2 was demonstrated when analogues 1-naphthol and nonylphenol were co-existed.   The imprinted factor and texture of the MIPs were contributed by PTMOS and APTES, respectively.   In addition, the optimal composition ratio of the MIPs was TEOS/APTES/PTMOS/MTMOS/E2=20/2/2/2/1. Increasing of TEOS/E2 or decreasing of TEOS/MTMOS ratios was not favor for adsorption ability due to decreased the density of recognition sites and the lack of rigid recognition sites, respectively.   The critical water/Si ratio of MIPs was 3.3.   The low adsorption capacity was resulted over or below the critical water/Si ratios due to the high affinity of APTES toward water or incompletely hydrolysis of the cross-linker.   However, incompletely hydrolysis promoted the imprinted factor by assisting the formation of imprinted cavities.   On the other hand, the adsorption capacity was decreased when the pH value was lower than 3 because the protonation of amino groups of APTES were weaken the interaction between the amino groups and E2.   In addition, HAc as catalyst disrupted the interaction between APTES and E2 by forming stronger hydrogen bonding with amino group than E2 to reduce the specific adsorption.   The rebinding ability was significantly determined by π-π stacking of PTMOS and specific surface areas of APTES.   The fast binding kinetic of MIPs was attributed to the high porosity of inorganic network.   Therefore, the appropriate functional monomers and adequate sol-gel parameters were crucial in preparation of organic-inorganic hybrid MIPs.

References

1. Wang, S.; Xu, Z. X.; Fang, G. Z.; Zhang, Y.; He, J. X., Separation and determination of estrone in environmental and drinking water using molecularly imprinted solid phase extraction coupled with HPLC. *Journal of Separation Science* **2008,** 31, (6-7), 1181-1188.

2. Zhang, Z. B.; Hu, J. Y., Selective removal of estrogenic compounds by molecular imprinted polymer (MIP). *Water Research* **2008,** 42, (15), 4101-4108.

3. Wang, S.; Huang, W.; Fang, G. Z.; Zhang, Y.; Qiao, H., Analysis of steroidal estrogen residues in food and environmental samples. *International Journal of Environmental Analytical Chemistry* **2008,** 88, (1), 1-25.

4. Saravanabhavan, G.; Helleur, R.; Hellou, J., GC-MS/MS measurement of natural and synthetic estrogens in receiving waters and mussels close to a raw sewage ocean outfall. *Chemosphere* **2009,** 76, (8), 1156-1162.

5. Bravo, J. C.; Fernandez, P.; Durand, J. S., Flow injection fluorimetric determination of beta-estradiol using a molecularly imprinted polymer. *Analyst* **2005,** 130, (10), 1404-1409.

6. Zhu, Q. J.; Tang, J.; Dai, J.; Gu, X. H.; Chen, S. W., Synthesis and characteristics of imprinted 17-beta-estradiol microparticle and nanoparticle with TFMAA as functional monomer. *Journal of Applied Polymer Science* **2007,** 104, (3), 1551-1558.

7. Bui, B. T. S.; Belmont, A. S.; Witters, H.; Haupt, K., Molecular recognition of endocrine disruptors by synthetic and natural 17 beta-estradiol receptors: a comparative study. *Analytical and Bioanalytical Chemistry* **2008,** 390, (8), 2081-2088.

8. Potyrailo, R. A.; Mirsky, V. M., Combinatorial and high-throughput development of sensing materials: The first 10 years. *Chemical Reviews* **2008,** 108, (2), 770-813.

9. Graham, A. L.; Carlson, C. A.; Edmiston, P. L., Development and characterization of molecularly imprinted sol-gel materials for the selective detection of DDT. *Analytical Chemistry* **2002,** 74, (2), 458-467.

10. Ye, L.; Weiss, R.; Mosbach, K., Synthesis and characterization of molecularly imprinted microspheres. *Macromolecules* **2000,** 33, (22), 8239-8245.

11. Szumski, M.; Buszewski, B., Molecularly imprinted polymers: A new tool for separation of steroid isomers. *Journal of Separation Science* **2004,** 27, (10-11), 837-842.

12. Watabe, Y.; Kubo, T.; Nishikawa, T.; Fujita, T.; Kaya, K.; Hosoya, K., Fully automated liquid chromatography-mass spectrometry determination of 17 beta-estradiol in river water. *Journal of Chromatography A* **2006,** 1120, (1-2), 252-259.

13. Jin, Y.; Jiang, M.; Shi, Y.; Lin, Y.; Peng, Y.; Dai, K.; Lu, B., Narrowly dispersed molecularly imprinted microspheres prepared by a modified precipitation polymerization method. *Analytica Chimica Acta* **2008,** 612, (1), 105-113.

14. Wei, S. T.; Molinelli, A.; Mizaikoff, B., Molecularly imprinted micro and nanospheres for the selective recognition of 17 beta-estradiol. *Biosensors & Bioelectronics* **2006,** 21, (10), 1943-1951.

15. Farrington, K.; Regan, F., Molecularly imprinted sol gel for ibuprofen: An analytical study of the factors influencing selectivity. *Talanta* **2009,** 78, (3), 653-659.

16. Silva, R. G. D.; Augusto, F., Sol-gel molecular imprinted ormosil for solid-phase extraction of methylxanthines. *Journal of Chromatography A* **2006,** 1114, (2), 216-223.

17. Diaz-Garcia, M. E.; Laino, R. B., Molecular imprinting in sol-gel materials: Recent developments and applications. *Microchimica Acta* **2005,** 149, (1-2), 19-36.

18. Gupta, R.; Kumar, A., Molecular imprinting in sol-gel matrix. *Biotechnology Advances* **2008,** 26, (6), 533-547.

19. Wei, H. S.; Tsai, Y. L.; Wu, J. Y.; Chen, H., Preparation of inorganic molecularly imprinted polymers with higher adsorption and selectivity by sol-gel method. *Journal of Chromatography B-Analytical Technologies in the Biomedical and Life Sciences* **2006,** 836, (1-2), 57-62.

20. Li, F.; Li, J.; Zhang, S. S., Molecularly imprinted polymer grafted on polysaccharide microsphere surface by the sol-gel process for protein recognition. *Talanta* **2008,** 74, (5), 1247-1255.

21. Nakada, N.; Shinohara, H.; Murata, A.; Kiri, K.; Managaki, S.; Sato, N.; Takada, H., Removal of selected pharmaceuticals and personal care products (PPCPs) and endocrine-disrupting chemicals (EDCs) during sand filtration and ozonation at a municipal sewage treatment plant. *Water Research* **2007,** 41, (19), 4373-4382.

22. Le Noir, M.; Plieva, F.; Hey, T.; Guieysse, B.; Mattiasson, B., Macroporous molecularly imprinted polymer/cryogel composite systems for the removal of endocrine disrupting trace contaminants. *Journal of Chromatography A* **2007,** 1154, (1-2), 158-164.

23. Ling, T. R.; Syu, Y. Z.; Tasi, Y. C.; Chou, T. C.; Liu, C. C., Size-selective recognition of catecholamines by molecular imprinting on silica-alumina gel. *Biosensors & Bioelectronics* **2005,** 21, (6), 901-907.

24. Ebarvia, B. S.; Binag, C. A.; Sevilla, F., Biomimetic piezoelectric quartz sensor for caffeine based on a molecularly imprinted polymer. *Analytical and Bioanalytical Chemistry* **2004,** 378, (5), 1331-1337.

25. Holthoff, E. L.; Bright, F. V., Molecularly templated materials in chemical sensing. *Analytica Chimica Acta* **2007,** 594, (2), 147-161.

26. Haupt, K.; Mosbach, K., Molecularly imprinted polymers and their use in biomimetic sensors. *Chemical Reviews* **2000,** 100, (7), 2495-2504.

27. Sellergren, B., Polymer- and template-related factors influencing the efficiency in molecularly imprinted solid-phase extractions. *Trac-Trends in Analytical Chemistry* **1999,** 18, (3), 164-174.

28. Cummins, W.; Duggan, P.; McLoughlin, P., A comparative study of the potential of acrylic and sol-gel polymers for molecular imprinting. *Analytica Chimica Acta* **2005,** 542, (1), 52-60.

29. Mayes, A. G.; Whitcombe, M. J., Synthetic strategies for the generation of molecularly imprinted organic polymers. *Advanced Drug Delivery Reviews* **2005,** 57, (12), 1742-1778.

30. Mahony, J. O.; Nolan, K.; Smyth, M. R.; Mizaikoff, B., Molecularly imprinted polymers-potential and challenges in analytical chemistry. *Analytica Chimica Acta* **2005,** 534, (1), 31-39.

31. Perez-Moral, N.; Mayes, A. G., Comparative study of imprinted polymer particles prepared by different polymerisation methods. *Analytica Chimica Acta* **2004,** 504, (1), 15-21.

32. Cormack, P. A. G.; Elorza, A. Z., Molecularly imprinted polymers: synthesis and characterisation. *Journal of Chromatography B-Analytical Technologies in the Biomedical and Life Sciences* **2004,** 804, (1), 173-182.

33. Spivak, D. A., Optimization, evaluation, and characterization of molecularly imprinted polymers. *Advanced Drug Delivery Reviews* **2005,** 57, (12), 1779-1794.

34. Sugahara, Y.; Inoue, T.; Kuroda, K., Si-29 NMR study on co-hydrolysis processes in Si(OEt)(4)-RSi(OEt)(3)-EtOH-water-HCl systems (R=Me,Ph): Effect of R groups. *Journal of Materials Chemistry* **1997,** 7, (1), 53-59.

35. Hunnius, M.; Rufinska, A.; Maier, W. F., Selective surface adsorption versus imprinting in amorphous microporous silicas. *Microporous and Mesoporous Materials* **1999,** 29, (3), 389-403.

36. Lee, S. W.; Ichinose, I.; Kunitake, T., Molecular imprinting of azobenzene carboxylic acid on a TiO2 ultrathin film by the surface sol-gel process. *Langmuir* **1998,** 14, (10), 2857-2863.

37. Hu, X. B.; Li, G. T.; Li, M. H.; Huang, J.; Li, Y.; Gao, Y. B.; Zhang, Y. H., Ultrasensitive specific stimulant assay based on molecularly imprinted photonic hydrogels. *Advanced Functional Materials* **2008,** 18, (4), 575-583.

38. Fang, G. Z.; Tan, J.; Yan, X. P., An ion-imprinted functionalized silica gel sorbent prepared by a surface imprinting technique combined with a sol-gel process for selective solid-phase extraction of cadmium(II). *Analytical Chemistry* **2005,** 77, (6), 1734-1739.

39. Wang, H. F.; Zhu, Y. Z.; Yan, X. P.; Gao, R. Y.; Zheng, H. Y., A room temperature ionic liquid (RTIL)-mediated, non-hydrolytic sol-gel methodology to prepare molecularly imprinted, silica-based hybrid monoliths for chiral separation. *Advanced Materials* **2006,** 18, (24), 3266-+.

40. Apperley, D.; Hay, J. N.; Raval, H. M., Silica-dimethylsiloxane hybrids-non-hydrolytic sol-gel synthesis and characterization by NMR spectroscopy. *Chemistry of Materials*

2002, 14, (3), 983-988.

41. Hayashi, K.; Yokota, Y.; Tachibana, T.; Kobashi, K.; Fukunaga, T.; Takada, T., Characteristics of diamond film gas sensors upon exposure to semiconductor doping gases. *Journal of the Electrochemical Society* **2001,** 148, (2), H17-H20.

42. Vioux, A., Nonhydrolytic sol-gel routes to oxides. *Chemistry of Materials* **1997,** 9, (11), 2292-2299.

43. Hsu, C. W.; Yang, M. C., Enhancement of the imprinting effect in cholesterol-imprinted microporous silica. *Journal of Non-Crystalline Solids* **2008,** 354, (34), 4037-4042.

44. Makote, R.; Collinson, M. M., Template recognition in inorganic-organic hybrid films prepared by the sol-gel process. *Chemistry of Materials* **1998,** 10, (9), 2440-2445.

45. Guardia, L.; Badia, R.; Diaz-Garcia, M. E., Molecular imprinted ormosils for nafcillin recognition by room temperature phosphorescence optosensing. *Biosensors & Bioelectronics* **2006,** 21, (9), 1822-1829.

46. Jin, G. Y.; Tang, Y. W.; Liu, S. Z.; Wang, S. C.; Xing, R. K., Preparation and application of a novel silica-supported organic-inorganic hybrid molecular imprinting polymer. *Analytical Letters* **2008,** 41, (10), 1811-1817.

47. Guardia, L.; Badia-Laino, R.; Diaz-Garcia, M. E.; Ania, C. O.; Parra, J. B., Role of surface adsorption and porosity features in the molecular recognition ability of imprinted sol-gels. *Biosensors & Bioelectronics* **2008,** 23, (7), 1101-1108.

48. Gao, N.; Xu, Z.; Wang, F.; Dong, S. J., Sensitive biomimetic sensor based on molecular imprinting at functionalized indium tin oxide electrodes. *Electroanalysis* **2007,** 19, (16), 1655-1660.

49. Fernandez-Gonzalez, A.; Laino, R. B.; Diaz-Garcia, M. E.; Guardia, L.; Viale, A., Assessment of molecularly imprinted sol-gel materials for selective room temperature phosphorescence recognition of nafcillin. *Journal of Chromatography B-Analytical Technologies in the Biomedical and Life Sciences* **2004,** 804, (1), 247-254.

50. Marx, S.; Liron, Z., Molecular imprinting in thin films of organic-inorganic hybrid sol-gel and acrylic polymers. *Chemistry of Materials* **2001,** 13, (10), 3624-3630.

51. Jin, G. Y.; Tang, Y. W., Evaluation of a novel silica-supported sol-gel sorbent prepared by a surface molecular imprinting technique for the selective separation of estazolam from human plasma. *Microchimica Acta* **2009,** 165, (1-2), 143-149.

52. Marx, S.; Zaltsman, A., Molecular imprinting of sol gel polymers for the detection of paraoxon in water. *International Journal of Environmental Analytical Chemistry* **2003,** 83, (7-8), 671-680.

53. Yang, H. H.; Zhang, S. Q.; Yang, W.; Chen, X. L.; Zhuang, Z. X.; Xu, J. G.; Wang, X. R., Molecularly imprinted sol-gel nanotubes membrane for biochemical separations. *Journal of the American Chemical Society* **2004,** 126, (13), 4054-4055.

54. Do Ki, C.; Oh, C.; Oh, S. G.; Chang, J. Y., The use of a thermally reversible bond for

molecular imprinting of silica spheres. *Journal of the American Chemical Society* **2002,** 124, (50), 14838-14839.

55. He, C. Y.; Long, Y. Y.; Pan, J. L.; Li, K.; Liu, F., Molecularly imprinted silica prepared with immiscible ionic liquid as solvent and porogen for selective recognition of testosterone. *Talanta* **2008,** 74, (5), 1126-1131.

56. He, C. Y.; Long, Y. Y.; Pan, J. L.; Li, K.; Liu, F., A method for coating colloidal particles with molecularly imprinted silica films. *Journal of Materials Chemistry* **2008,** 18, (24), 2849-2854.

57. Jin, G. Y.; Li, W.; Yu, S. N.; Peng, Y. Y.; Kong, J. L., Novel superparamagnetic core-shell molecular imprinting microspheres towards high selective sensing. *Analyst* **2008,** 133, (10), 1367-1372.

58. Jiang, X. M.; Tian, W.; Zhao, C. D.; Zhang, H. X.; Liu, M. C., A novel sol-gel-material prepared by a surface imprinting technique for the selective solid-phase extraction of bisphenol A. *Talanta* **2007,** 72, (1), 119-125.

59. Zhang, Y.; Qin, Z.; Tu, Z. Y., Study of the preparation of flavone imprinted silica microspheres and their molecular recognition function. *Chemical Engineering & Technology* **2007,** 30, (8), 1014-1019.

60. Xie, C. G.; Liu, B. H.; Wang, Z. Y.; Gao, D. M.; Guan, G. J.; Zhang, Z. P., Molecular imprinting at walls of silica nanotubes for TNT recognition. *Analytical Chemistry* **2008,** 80, (2), 437-443.

61. Xu, Z. X.; Chen, S.; Huang, W.; Fang, G. Z.; Hua, P. Z.; Wang, S., Study on an on-line molecularly imprinted solid-phase extraction coupled to high-performance liquid chromatography for separation and determination of trace estrone in environment. *Analytical and Bioanalytical Chemistry* **2009,** 393, (4), 1273-1279.

62. Skrdla, P. J.; Shnayderman, M.; Wright, L.; O'Brien, T. P., GC-MS study of the formation of alkoxysilanes from a sol-gel precursor in a hydrophobic solution: A potential new route to hybrid molecular imprinted polymers. *Journal of Non-Crystalline Solids* **2006,** 352, (30-31), 3302-3309.

63. Moreau, J. J. E.; Man, M. W. C., The design of selective catalysts from hybrid silica-based materials. *Coordination Chemistry Reviews* **1998,** 180, 1073-1084.

64. Lin, C. I.; Joseph, A. K.; Chang, C. K.; Wang, Y. C.; Lee, Y. D., Synthesis of molecular imprinted organic-inorganic hybrid polymer binding caffeine. *Analytica Chimica Acta* **2003,** 481, (2), 175-180.

65. Chen, Z. F.; Liu, Y. C.; Liu, L. M.; Wang, H. S.; Qin, S. H.; Wang, B. L.; Bian, H. D.; Yang, B.; Fun, H. K.; Liu, H. G.; Liang, H.; Orvig, C., Potential new inorganic antitumour agents from combining the anticancer traditional Chinese medicine (TCM) liriodenine with metal ions, and DNA binding studies. *Dalton Transactions* **2009**, (2), 262-272.

66. Olwill, A.; Hughes, H.; O'Riordain, M.; McLoughlin, P., The use of molecularly

imprinted sol-gels in pharmaceutical separations. *Biosensors & Bioelectronics* **2004,** 20, (6), 1045-1050.

67. Feng, L.; Liu, Y. J.; Zhou, X. D.; Hu, J. M., The fabrication and characterization of a formaldehyde odor sensor using molecularly imprinted polymers. *Journal of Colloid and Interface Science* **2005,** 284, (2), 378-382.

68. Matsuguchi, M.; Uno, T., Molecular imprinting strategy for solvent molecules and its application for QCM-based VOC vapor sensing. *Sensors and Actuators B-Chemical* **2006,** 113, (1), 94-99.

69. Jimenez-Cadena, G.; Riu, J.; Rius, F. X., Gas sensors based on nanostructured materials. *Analyst* **2007,** 132, (11), 1083-1099.

70. Kong, J.; Franklin, N. R.; Zhou, C. W.; Chapline, M. G.; Peng, S.; Cho, K. J.; Dai, H. J., Nanotube molecular wires as chemical sensors. *Science* **2000,** 287, (5453), 622-625.

71. Marx, S.; Zaltsman, A.; Turyan, I.; Mandler, D., Parathion sensor based on molecularly imprinted sol-gel films. *Analytical Chemistry* **2004,** 76, (1), 120-126.

72. Wen, W.; He, S. T.; Li, S. Z.; Liu, M. H.; Yong, P., Enhanced sensitivity of SAW gas sensor coated molecularly imprinted polymer incorporating high frequency stability oscillator. *Sensors and Actuators B-Chemical* **2007,** 125, (2), 422-427.

73. Fu, Y.; Finklea, H. O., Quartz crystal microbalance sensor for organic vapor detection based on molecularly imprinted polymers. *Analytical Chemistry* **2003,** 75, (20), 5387-5393.

74. Ji, H. S.; McNiven, S.; Lee, K. H.; Saito, T.; Ikebukuro, K.; Karube, I., Increasing the sensitivity of piezoelectric odour sensors based on molecularly imprinted polymers. *Biosensors & Bioelectronics* **2000,** 15, (7-8), 403-409.

75. Tsuru, N.; Kikuchi, M.; Kawaguchi, H.; Shiratori, S., A quartz crystal microbalance sensor coated with MIP for "bisphenol A" and its properties. *Thin Solid Films* **2006,** 499, (1-2), 380-385.

76. Le Noir, M.; Plieva, F. M.; Mattiasson, B., Removal of endocrine-disrupting compounds from water using macroporous molecularly imprinted cryogels in a moving-bed reactor. *Journal of Separation Science* **2009,** 32, (9), 1471-1479.

77. Xu, F. X.; Koch, D. E.; Kong, I. C.; Hunter, R. P.; Bhandari, A., Peroxidase-mediated oxidative coupling of 1-naphthol: Characterization of polymerization products. *Water Research* **2005,** 39, (11), 2358-2368.

78. Elkins, C. A.; Mullis, L. B., Mammalian steroid hormones are substrates for the major RND- and MFS-type tripartite multidrug efflux pumps of Escherichia coli. *Journal of Bacteriology* **2006,** 188, (3), 1191-1195.

79. Mansell, J.; Drewes, J. E.; Rauch, T., Removal mechanisms of endocrine disrupting compounds (steroids) during soil aquifer treatment. *Water Science and Technology* **2004,** 50, (2), 229-237.

80. Gupta, M. N.; Batra, R.; Tyagi, R.; Sharma, A., Polarity index: The guiding solvent parameter for enzyme stability in aqueous-organic cosolvent mixtures. *Biotechnology Progress* **1997,** 13, (3), 284-288.

81. Le Noir, M.; Lepeuple, A. S.; Guieysse, B.; Mattiasson, B., Selective removal of 17 beta-estradiol at trace concentration using a molecularly imprinted polymer. *Water Research* **2007,** 41, (12), 2825-2831.

82. Nony, L.; Boisgard, R.; Aime, J. P., DNA properties investigated by dynamic force microscopy. *Biomacromolecules* **2001,** 2, (3), 827-835.

83. Dong, H.; Tong, A. J.; Li, L. D., Syntheses of steroid-based molecularly imprinted polymers and their molecular recognition study with spectrometric detection. *Spectrochimica Acta Part a-Molecular and Biomolecular Spectroscopy* **2003,** 59, (2), 279-284.

84. He, L.; Powers, K.; Baney, R. H.; Gower, L.; Duran, R. S.; Sheth, P.; Carino, S. R., Mesoporous TMOS-MTMS copolymer silica gels catalyzed by fluoride. *Journal of Non-Crystalline Solids* **2001,** 289, (1-3), 97-105.

85. Husing, N.; Schubert, U.; Mezei, R.; Fratzl, P.; Riegel, B.; Kiefer, W.; Kohler, D.; Mader, W., Formation and structure of gel networks from Si(OEt)(4)/(MeO)(3)Si(CH2)(3)NR '(2) mixtures (NR '(2) = NH2 or NHCH2CH2NH2). *Chemistry of Materials* **1999,** 11, (2), 451-457.

86. Gommes, C. J.; Basiura, M.; Goderis, B.; Pirard, J. P.; Blacher, S., Structure of silica xerogels synthesized with organoalkoxysilane co-reactants hints at multiple phase separation. *Journal of Physical Chemistry B* **2006,** 110, (15), 7757-7765.

87. Tarafdar, A.; Biswas, S.; Pramanik, N. K.; Pramanik, P., Synthesis of mesoporous chromium phosphate through an unconventional sol-gel route. *Microporous and Mesoporous Materials* **2006,** 89, (1-3), 204-208.

88. Chang, Y. S.; Ko, T. H.; Hsu, T. J.; Syu, M. J., Synthesis of an Imprinted Hybrid Organic-Inorganic Polymeric Sol-Gel Matrix Toward the Specific Binding and Isotherm Kinetics Investigation of Creatinine. *Analytical Chemistry* **2009,** 81, (6), 2098-2105.

89. Huang, S. J.; Lee, H. K.; Lee, Y. S.; Kang, W. H., Proton-conductive membranes doped with orthophosphoric acid based on inorganic-organic hybrid materials. *Journal of the American Ceramic Society* **2005,** 88, (12), 3427-3432.

90. Wang, X. G.; Tseng, Y. H.; Chan, J. C. C.; Cheng, S. F., Catalytic applications of aminopropylated mesoporous silica prepared by a template-free route in flavanones synthesis. *Journal of Catalysis* **2005,** 233, (2), 266-275.

91. Lee, S. C.; Lin, H. M.; Chen, H., Studies on the Preparation and Properties of Inorganic Molecularly Imprinted Polymer (MIP) Based on Tetraethoxysilane and Silane Coupling Agents. *Journal of Applied Polymer Science* **2009,** 114, (6), 3994-3999.

92. Fujiwara, M.; Nishiyama, M.; Yamamura, I.; Ohtsuki, S.; Nomura, R., A sol-gel method

using acetic anhydride in the presence of cholesterol in organic solution media: Preparation of silicas that recognize steroid hormones. *Analytical Chemistry* **2004,** 76, (8), 2374-2381.

Appendix A.   Extraction test

The extraction test was performed by Soxhlet apparatus or stirred in hot plate accompanied with three kinds of solvent types including methanol, acidic methanol, and hot methanol showed in Table A-1.   For Soxhlet apparatus, 300 ml of solvent was used and heated for 24 hr.   Stirring in hot plate was employed 40 ml of solvent at 200 rpm for 4 hr through 12 times for extraction.   The "release" in table means the extraction incomplete and some template still released from sample.

Table A-1. Compared with soxhlet and hot plate for extraction test.

	Methanol	**Methanol with acetic acid (10% v/v)**	**Hot methanol (85 ^{o}C)**
Soxhlet	Release	Release	No detected
Hot plate	Release	Release	No release

According to the Table A-1, the best solution for removal of template from imprinted polymers was continuous stirred in hot plate used hot methanol.   This is because the structure of template was bigger and difficult removal from rigid network of silica.   Hot methanol could disrupt the interaction between the template and imprinted polymers, and decreased the surface tension.   In addition, vigorous stirring could increase the contacted opportunity between template and imprinted polymers.

Appendix B. Sieved test

In order to demonstrate the all adsorption result under saturated equilibrium, the low porosity of TAPMc and high organic substituted T2 were selected for adsorption equilibtium where composition of T2 was the TEOS /APTES/PTMOS/MTMOS/E2 molar ratio controlled at 2/20/2/2/1. This was because the low porosity of material with low diffusion rate could not achieve saturation state. The adsorption kinetic of TAPMc and T2 were showed in Figure B-1. Both of samples were reached equilibrium in four hr. So, it was demonstrated that all adsorption results were performed on saturation equilibrium.
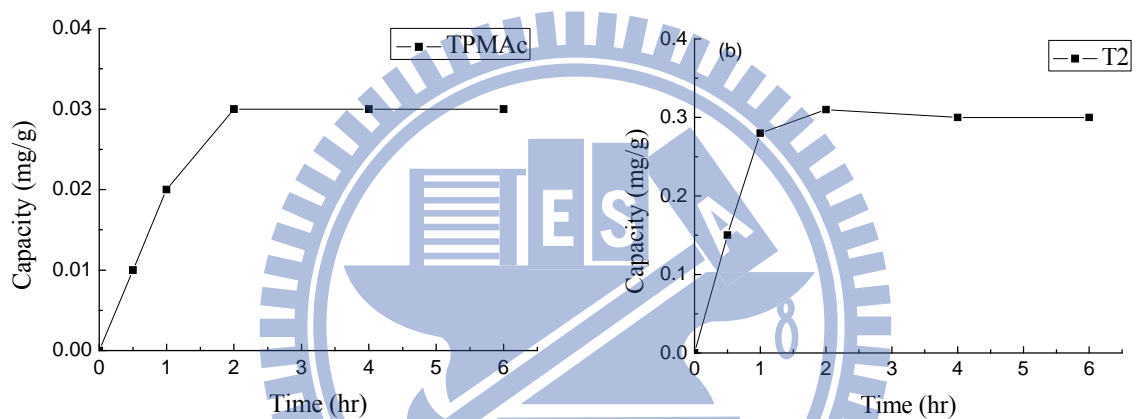

Figure B-1. The adsorption capacities of TAPMc and T2 toward E2 in the regular time intervals ranged from 30 min to 6 hr.

On the other hand, the sieved test was carried out for understanding the effect of particle size on adsorption capacity and porosity. The sieved process was collected samples through the stainless steel sieves between mesh numbers of 200 and 325, which correspond to 75 and 25 μ m diameter. The adsorption capacity and porosity of TAPMc and T2 with and without sieving were shown in Table B-1. After sieved process, the adsorption capacity of TAPMc was decreased from 0.015 to 0.01 mg/g, and the specific surface areas also decreased from 34.7 m^2/g to 30.2 m^2/g; whereas the adsorption capacity of T2 was slightly increased from 0.3 mg/g to 0.32 mg/g, and the specific surface areas was decreased from 431.5 m^2/g to 425.2

m^2/g.   There was not significantly different on adsorption and porosity after sieved process. This was due to fast gelation process by using APTES.   The fast gelation caused the small particles.   Besides, the organic incorporated into silica matrix would generate the steric effect that decrease the opportunity between particles.   In this way, small particle was easy formation.

Table B-1. The adsorption capacity and BET results of TAPMc and T2 for sieved test.

Sample	K$_d$ (mg/g)	Specific surface areas (m^2/g)	Pore volume (cm^3/g)
TAPMc before sieving	0.015	34.7	0.43
TAPMc after sieving	0.01	30.2	0.33
T2 before sieving	0.3	431.5	1.06
T2 after sieving	0.32	425.2	0.98
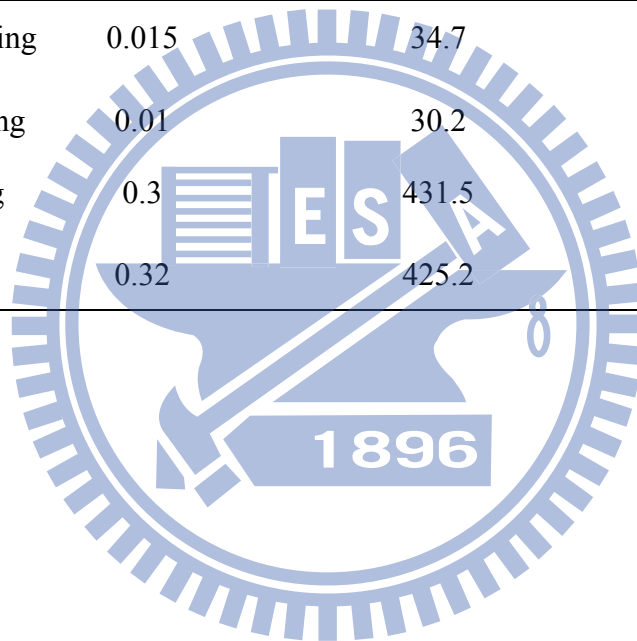
Appendix C.　Covalent bond

We used a thermally cleavable urethane bond for covalent bond test according to Chang's groups.[54] The thermally cleavable bond was stable at room temperature and cleavage at elevated temperature. The covalent bond between the monomer and template complex was synthesized herein for comparing with non-covalent interactions by instead of 3-isocyanatopropyltriethoxysilane (ICPS) as functional group of imprinted polymers. The thermally reversible reaction was occurred between the isocyanate group of ICPS and a phenol moiety of E2 showed in Figure 3-3. The sample of ICPS was synthesized in the same procedure with the sample APTES, but the functional group was used ICPS to replace APTES, which used in the sample APTES. The adsorption capacity of covalent (ICPS) and non-covalent (APTES) were showed in Figure C-1. The adsorption capacities were 0.23 mg/g for ICPS and 0.45 mg/g for APTES. The imprinted factor was 2.9 for ICPS and 1.6 for APTES. The adsorption capacity of ICPS was lower than APTES due to reduction of cavities. The result was because that the reversible urethane bond was incompletely occurred in preparation process by chemical reaction. However, the imprinted factor of sample ICPS was better than sample APTES because of good recognition sites. Therefore, the complementary cavities formation by ICPS was more suitable for E2 than APTES due to high imprinted factor. The few templates could be removed and decreased the recognition sites.
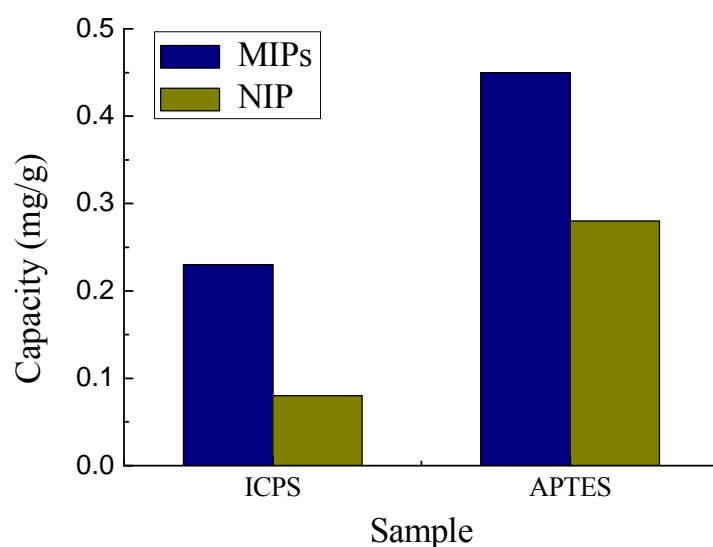
Figure C-1. The adsorption capacity for covalent (ICPS) and non-covalent (APTES) bond.

Before and after extraction of E2 for ICPS was showed in Figure C-2 by means of IR spectroscopy measurements. The carbonyl peak attributed to urethane bond between template and ICPS was appeared at 1736 cm^{-1} before extraction, and was decreased after extraction.[53] This was illustrated that the urethane bond formed after chemical reaction but it was inconspicuous. In addition, the amino group around 1432-1642 cm^{-1} was appeared in sample after extraction due to the conversion of urethane bond.
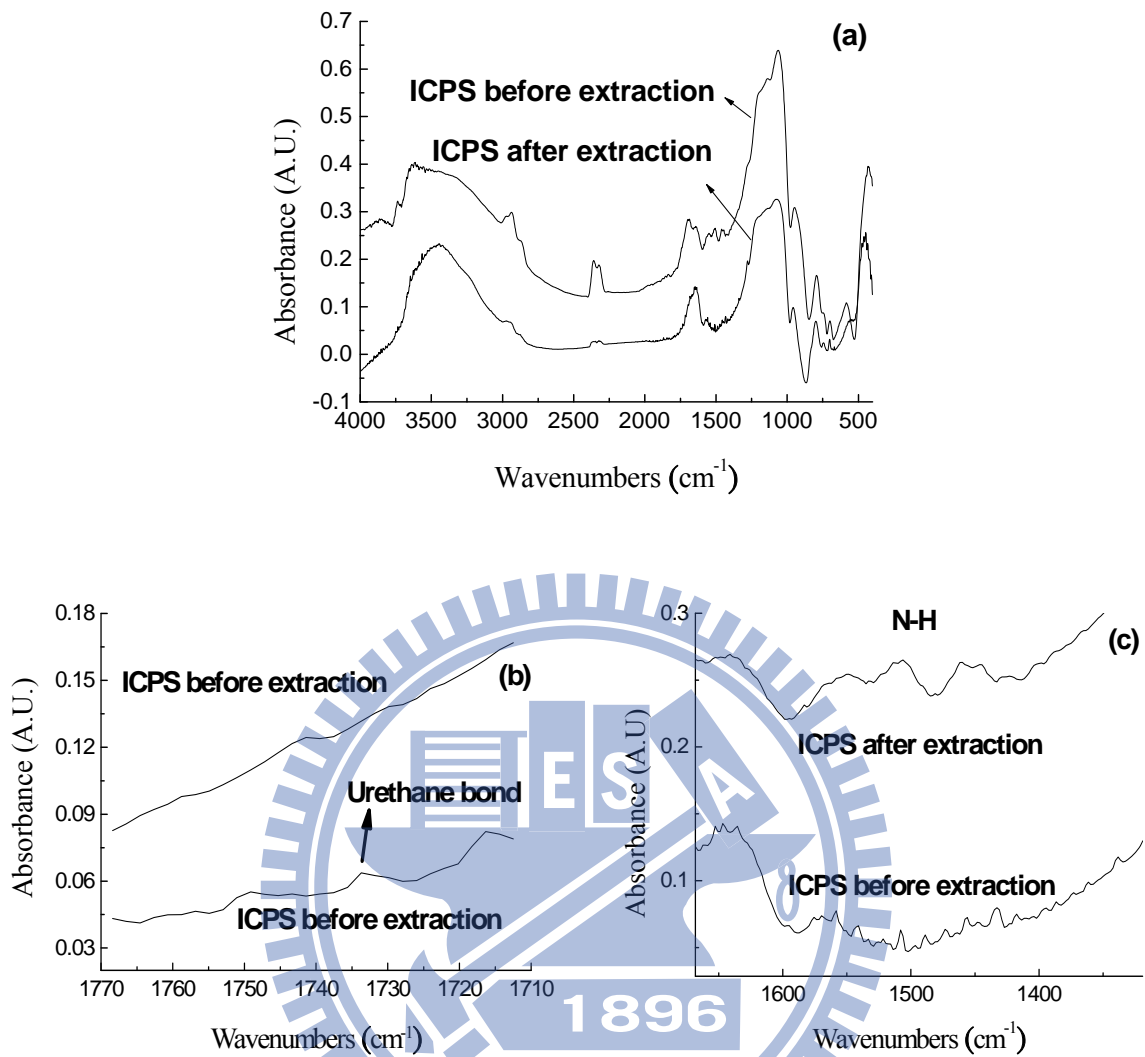
Figure C-2. IR spectra of ICPS before and after extraction with wavenumbers (a)4000-400 cm^{-1}, (b)1170-1710 cm^{-1}, and (c) 1650-1350 cm^{-1}.

It should be note that the specific surface areas of ICPS before extraction was 1 m^2/g and 2 m^2/g for its correspond NIP. After extraction process, the specific surface areas were increased from 1 m^2/g to 691 m^2/g for ICPS and from 2 m^2/g to 589 m^2/g for NIP. This is because many amount of ICPS functional group unable to bond to E2 in solution. Following, the silanol groups of hydrolyzed precursor may react to ICPS functional group in gelation process and formed the network. Therefore, the extraction process would remove the ICPS functional group from network and increased the specific surface areas. The

specific surface areas of both ICPS and related NIP were increased significantly.   Besides, the specific surface areas of ICPS was slight large than related NIP due to the removal of template.   In addition, the low adsorption capacity was presented due to the small amount amino group which was converted from ICPS functional group.   For this reason, the imprinted cavity and corresponding functional group were played an important role on recognition of target molecule.

Table C-1. Profiles of ICPS and related control polymer (NIP) for extraction effects test.

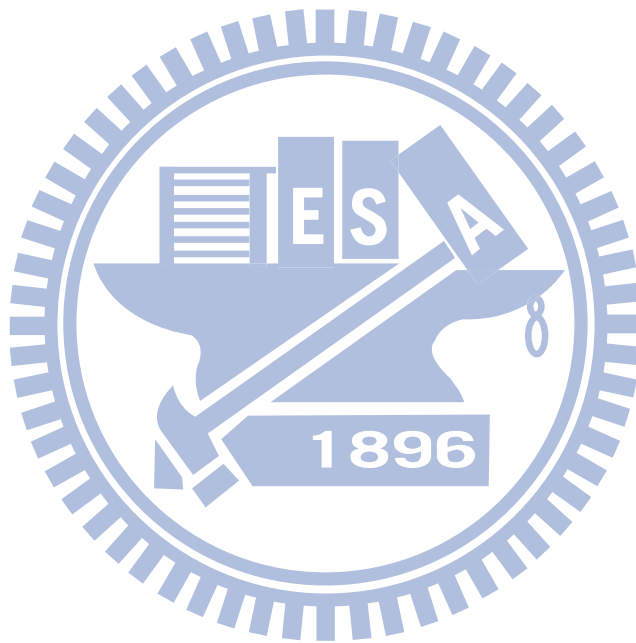| Samples		Specific surface areas (m^2/g)	Pore volume (cm^3/g)
ICPS	before extraction	1	0.01
	after extraction	691	0.40
NIP	before extraction	2	0.01
	after extraction	589	0.32

Appendix D.   Apparatus

Table D-1. The apparatus used in this study.

No.	Apparatus	Type	Brand
1	Balance	AB204-S	METTLER TOLEDO
2	Compact centrifuge	CF15RXII	HITACHI
3	Shaker	Vortex-Genie 2	Scientific Industries
4	Hot plate/stirrer (for preparation)	HP-240	NORTH WORLD
5	Hotplate stirrer (for extraction)	C-MAG HS7 S26	IKA
6	High temperature oven	Vulcan 3-550 Furnace	Densply